NASA Contractor Report 3469

Selected Advanced Aerodynamic and Active Control Concepts Development

Summary Report

Staff of Douglas Aircraft Company

CONTRACT NAS1-14744
OCTOBER 1981

NASA

NASA Contractor Report 3469

Selected Advanced Aerodynamic and Active Control Concepts Development

Summary Report

Staff of Douglas Aircraft Company
McDonnell Douglas Corporation
Long Beach, California

Prepared for
Langley Research Center
under Contract NAS1-14744

National Aeronautics
and Space Administration

**Scientific and Technical
Information Branch**

1981

FOREWORD

This document summarizes contract work performed for the NASA Energy Efficient Transport (EET) project of the Aircraft Energy Efficiency (ACEE) program by the Douglas Aircraft Company.

The NASA EET Project Manager was, first, W. J. Alford, then R. V. Hood of the Energy Efficient Transport Project Office at the Langley Research Center. D. L. Maiden was technical monitor. The NASA on-site representative was J. R. Tulinius. The principal Douglas Aircraft Company personnel responsible for the work described in this report were:

M. Klotzsche	ACEE Program Manager	
A. B. Taylor	EET Project Manager	
D. K. Steckel	Aerodynamics Engineering (High-Aspect-Ratio Supercritical Wing High-Speed Development)	
W. R. Oliver	Aerodynamics Engineering (High-Aspect-Ratio Supercritical Wing High-Lift Development)	
Dr. C. A. Shollenberger	Aerodynamics Engineering (Study of a Transport Configuration with a Supercritical Wing and Winglet)	
T. R. Sizlo	Avionics Engineering	Relaxed Static Stability and Augmentation System Study
R. A. Berg	Aerodynamics Engineering	
D. L. Gilles	Reliability and Safety Engineering	
W. A. Shirley	Advanced Engineering (Aerodynamics Performance of an Aileron for Active Control)	

CONTENTS

SUMMARY

This report summarizes investigations and experimental development in aerodynamics and active controls specifically applicable to an advanced medium-range commercial transport. The baseline against which the work was performed and evaluated was the Douglas DC-X-200 twin-engine derivative of the DC-10 transport.

In aerodynamics, the primary emphasis was on the design of high-aspect-ratio supercritical wings which, in conjunction with an advanced high-lift system, could meet the design goals of the aircraft in terms of cruise drag, buffet boundary, and off-design performance. Nacelles and pylons, flap support fairings, ailerons, and tail surfaces were also tested. The results of the development of the cruise-speed configuration support initial predictions that significant reductions in fuel burned and direct operating costs, compared with those of current conventional wing configurations, can be realized. Low-speed experimental work resulted in the development of substantial advances in high-lift technology for this class of wing relative to the previous data in three dimensions at high Reynolds number. Important improvements in high-lift performance compared with current standards were demonstrated. The experimental results include the effects of various leading- and trailing-edge devices, nacelles and pylons, aileron, spoilers, and Mach and Reynolds numbers. In both high-speed and high-lift work, satisfactory correlation was obtained between experiment and advanced computational and design methods.

Using supercritical wing technology, a preliminary design study resulted in an aircraft design which from the initial stages employed an integrated wing and winglet lift system. The design was compared with the baseline aircraft having only a supercritical wing, and it was determined that the wing-winglet combination could confer advantages in weight and fuel economy. These indications were sensitive to the impact of flutter characteristics and, to a lesser extent, the performance of the high-lift system.

Active control work was concentrated on the determination of criteria, configuration, and flying qualities associated with augmented longitudinal stability of a level likely to be acceptable for the next-generation transport, and on the design of a practical augmentation system. Motion base simulation of the unaugmented and augmented aircraft determined permissible stability margins. It was found acceptable to incorporate a more negative static margin than the neutral stability assumed for the original unaugmented

baseline. Further fuel economy could therefore be assured for a modified baseline. Simple control laws were found to be adequate to supply the required qualities for the augmented aircraft. Candidate system architectures were defined based on detailed requirements including reliability and safety.

Additional work related to active controls determined aerodynamic data for separate studies of wing load alleviation and elastic mode control for the DC-10. The performance and potential limitations of the existing aileron surfaces were defined.

Recommendations for continuing to expand the technology base were made. It was concluded that although substantial progress had been made in the supercritical wing technology, the potential exists for further improvements. Additional experimental programs were suggested. A successful conclusion to these would enable more specific proposals to be made for wing-winglet combination concepts. It was concluded that the current work on stability augmentation was being done at a level satisfactory for detail design application. The direction of further work should be in the area of elastic model control.

INTRODUCTION

By the nature of market pressures, replacements for the current medium-range transports require substantial technical advances. This market contains the greatest quantity of aircraft and is therefore the largest user of fuel. It has long been clear that significant technical advances addressing fuel efficiency (now becoming even more important to market success) are needed. At the same time, the introduction of new technology must be guided by sound economic guidelines and technical acceptance by operators and regulatory bodies.

Studies at Douglas for medium-range transports (generically called "advanced commercial aircraft") had, prior to the inception of the NASA Energy Efficient Transport project, focused on the DC-X-200 design. The twin-engined DC-X-200 was a major derivative of the DC-10, itself an energy-efficient transport of its generation. This design reflected a number of advanced features and generated attractive performance.

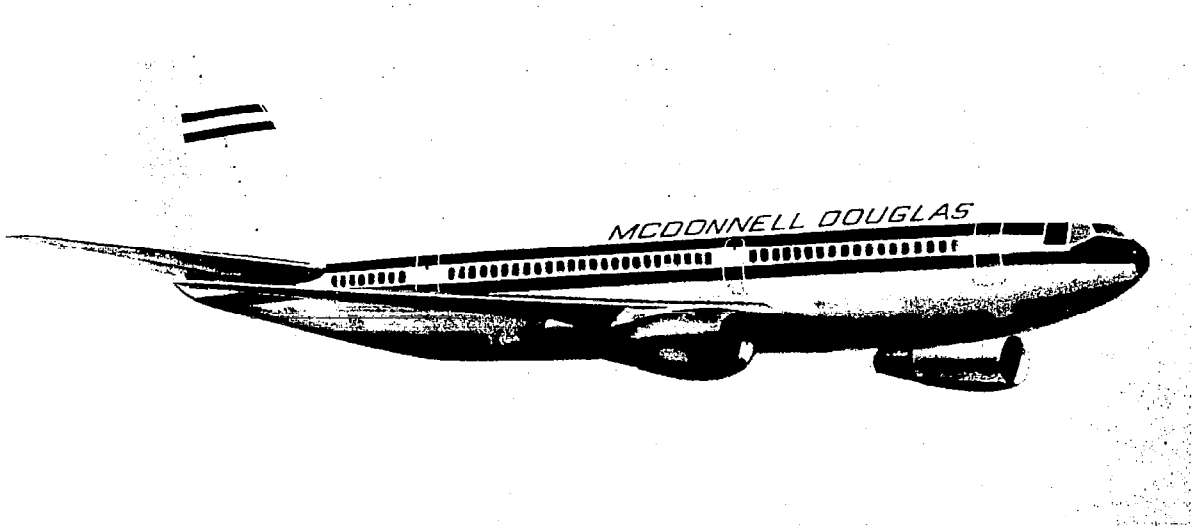

DOUGLAS DC-X-200 TRANSPORT

During the time of the DC-X-200 studies, the NASA Aircraft Energy Efficiency (ACEE) program was introduced to accelerate the incorporation of new technology. From this program, the Energy Efficient Transport (EET) project was directed toward the application of advanced aerodynamics and active controls. The relationship of the two activities was beneficial for a sound advancement of technology, since EET development could be backed by detailed studies on the DC-X-200.

The subsequent selection of EET tasks encompassed the following:

- Aerodynamics: The design and wind tunnel development of high-aspect-ratio supercritical wings, investigating both the cruise speed and high-lift.

- Configuration Design: The preliminary design and evaluation of an aircraft combining a high-aspect-ratio supercritical wing with a winglet.

- Active Controls: The determination of criteria, configuration, and flying qualities associated with augmented longitudinal stability of a level likely to be acceptable for the next-generation transport, and the design of a practical augmentation system.

The gains predicted for these concepts can be evaluated in a number of ways. Two simple but effective measures are the improvements in direct operating cost (DOC) and fuel use. DOC is one measure of the economics of the aircraft to which the particular technology concept contributes, and fuel use is a powerful ingredient of this figure. Owing to the increasing importance of fuel conservation, the fuel use measure is of interest in its own right.

The true quantification of the predicted gains involves a complete aircraft configuration analysis in which the relationships of all the factors may be represented. However, the effects of each concept noted independently can provide an approximation of the net value for the DC-X-200 aircraft as a whole.

Concept	Percent Reduction Relative to DC-10 Technology DOC	Fuel Burned
High-Aspect-Ratio Supercritical Wing	4.5	9.0
High-Aspect Ratio	(1.0)	(4.0)
Supercritical Wing	(3.5)	(5.0)
Advanced High-Lift System	1.9	1.5
Augmented Stability	0.5	2.8

These improvements were considered most substantial, warranting vigorous development. Additional inducements were recognized in the field of high-lift development, owing to its potential for improving field length and reducing community noise.

The combination of the advanced wing and winglet in a new aircraft was estimated in the study to result in an improvement over the DC-X-200 of 0.7 percent in DOC and 1.5 percent in fuel burned.

After the inception of the tasks previously introduced, an additional task was performed. This task investigated the aerodynamic behavior of the outboard aileron of the DC-10 transport under conditions which would be appropriate for its use as an active control surface. The wind tunnel test results of this task are summarized in this report.

The use of trade names or names of manufacturers in this report does not constitute an official endorsement of such products or manufacturers, either expressed or implied, by the National Aeronautics and Space Administration.

SYMBOLS

Dimensional values referring to test data and results are presented in both the International System of Units (SI) and U.S. Customary Units.

A_N	aircraft normal acceleration
A_x	aircraft longitudinal acceleration
ADC	air data computer
AR	aspect ratio
C_D	coefficient of drag
C_L	coefficient of lift
C_l	section lift coefficient
C_m	pitching moment
CG	center of gravity
DOC	direct operating cost
L/D	lift to drag ratio
M	Mach number
MAC	mean aerodynamic chord
Q	failure probability
R	Reynolds number
$R_{\bar{c}}$	Reynolds number at mean aerodynamic chord
RBM	wing root bending moment
RSSAS	Relaxed static stability augmentation system
V_D	dive speed
V_F	flutter speed
V_S	stalling speed (the minimum aircraft speed at which the aircraft is controllable)
VCK	variable camber Krueger flap
b	wing span
$\bar{c}/4$	one quarter point of the mean aerodynamic chord
$\dot{h}$	altitude rate

i_H	incidence angle between horizontal tail and the fuselage reference plane, positive trailing edge down (degrees)
t/c	airfoil thickness chord ratio
v	aircraft velocity
ΔC_{D_C}	compressibility drag coefficient increment
α	angle of attack
δ_F	flap deflection
$\delta_{F_{EFF}}$	effective flap deflection
ε	drag efficiency factor
θ/θ_c	closed-loop resonance
$\dot{\theta}$	aircraft pitch rate
$\ddot{\theta}$	aircraft pitch acceleration
σ_w	RMS gust velocity

BASELINE AIRCRAFT

The aircraft used as a basis for the design investigations reported in this summary report was the subject of Douglas Aircraft Company studies for medium-range transports. These aircraft were generically called "advanced commercial aircraft," but at the time of the EET project the configuration family was entitled the DC-X-200. From time to time during the project, the DC-X-200 definition was modified slightly as the design studies progressed. These changes are not considered to have affected the EET development tasks or results in any significant way. Where appropriate, however, specific configuration comparisons are identified in the specific summary areas. The representative baseline definition is described below.

General Arrangement

The general arrangement of the baseline aircraft is shown in the accompanying illustration. Featured are a shortened DC-10 fuselage of 230-seat nominal capacity, a new high-aspect-ratio advanced-technology wing, and two underwing-mounted turbofan engines. The major components retained from the DC-10, in addition to the modified fuselage structure, include the engine pods, the nose landing gear, and major portions of the aircraft systems. New components, in addition to the advanced wing, are the empennage, the flight guidance and control system, the engine pylons, and the main landing gear.

Advanced Features

The design definition reflects incorporation of advanced-technology features that contributed to improved economics chiefly by reduced consumption. The most noteworthy feature is the thick high-aspect-ratio wing with supercritical sections. This wing is combined with an advanced high-lift system — variable camber Krueger leading-edge devices and a two-segment trailing-edge flap. In addition, reduced static stability with stability augmentation is incorporated. Other features include electrically signalled spoilers; digital flight guidance and control; improved thrust control; and composite-structure floor beams and struts, control surfaces, wing fixed trailing edges, and wing body and tail fairings.

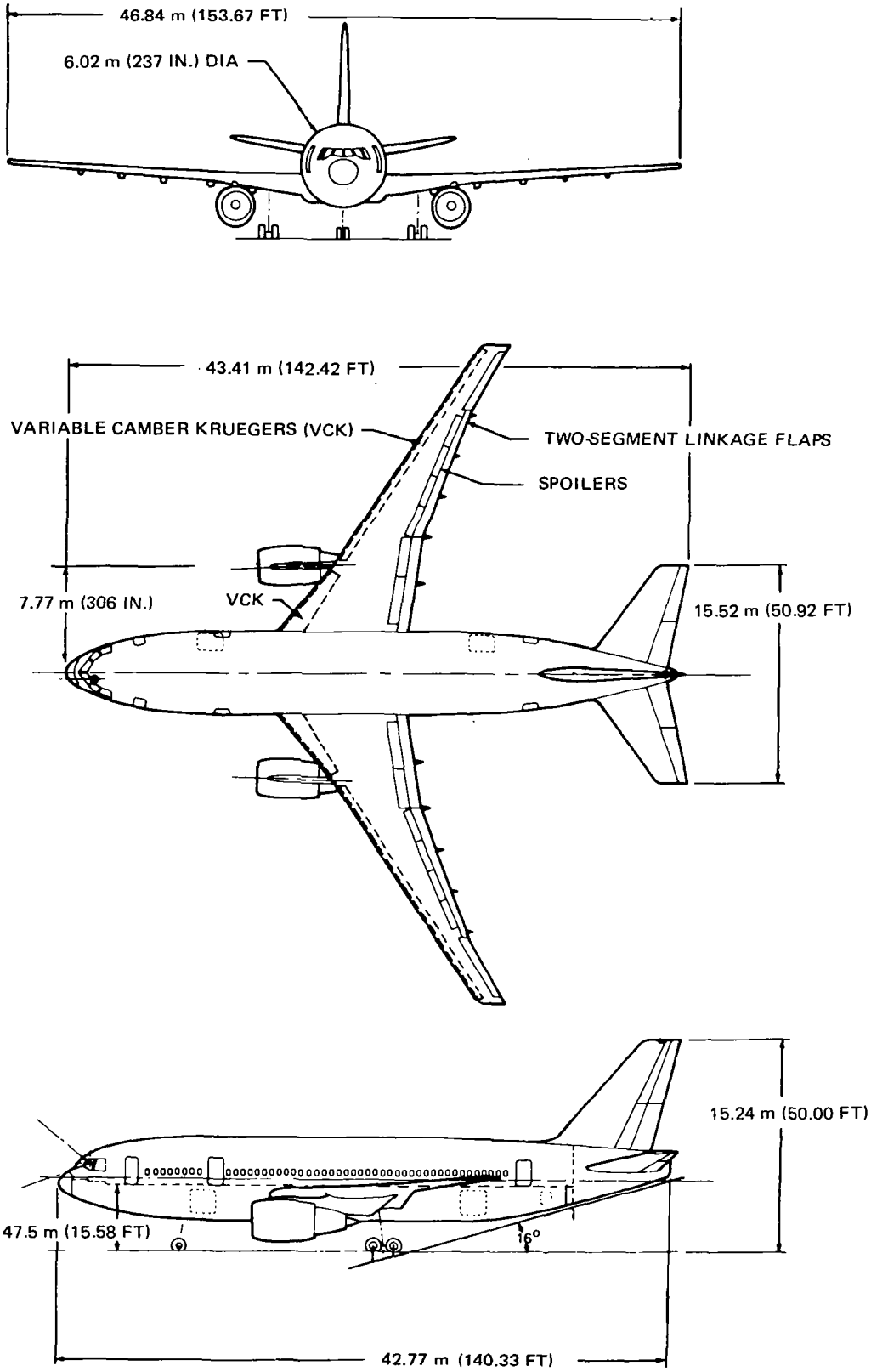

BASELINE DC-X-200 GENERAL ARRANGEMENT

Weight Summary

The baseline is defined by the following weights:

Maximum ramp	133,809 kg (295,000 lb)
Maximum takeoff	132,902 kg (293,000 lb)
Maximum landing	117,934 kg (260,000 lb)
Maximum zero fuel	112,944 kg (249,000 lb)
Operator's empty weight	79,038 kg (174,250 lb)
Maximum payload	33,906 kg (74,750 lb)

Mission and Other Requirements

The aircraft is designed for a passenger payload of 21,390 kg (47,150 lb) at a range of 5,844 km (2,620 n mi). The payload is equivalent to 230 passengers and their baggage. The range is defined with FAR domestic reserves, using a 446-km (200-n-mi) alternate. The initial cruise altitude requirement is 10,363 m (34,000 ft). Initial cruise Mach number is 0.80. The approach speed requirement is 241 km/hr (130 kn) or less. General Electric CF6-45 engines, rated at 200.16 kN (45,000 lb) sea level static thrust, are specified.

A number of evaluations in the EET studies were performed for a block distance of 1,389 km (750 n mi). This mission is typical of a large class of operations.

HIGH-ASPECT-RATIO SUPERCRITICAL WING HIGH-SPEED DEVELOPMENT*

Objective

The objective of this task was to develop and extend the aerodynamic technology base for high-aspect-ratio supercritical wings.

Approach

A basic wing was designed based on contractor in-house system studies. Variations, primarily in wing leading- and trailing-edge geometry, were then developed. The alternative configurations were tested in the wind tunnel in order to:

- Determine the effects of geometry changes on wing performance
- Determine the interference effects of nacelles and pylons and of flap linkage fairings
- Evaluate theoretical and semiempirical estimation techniques.

Wing Configuration Development

In the development of the wing geometry, heavy reliance was placed on two- and three-dimensional test data generated by both Douglas and NASA as well as on advanced computational methods.

*The contract work is reported in detail in the document of Reference 1.

The study baseline wing configuration was a high-aspect-ratio wing with a large inboard trailing-edge extension to house the landing gear. This wing closely resembled two previously developed configurations which had been wind-tunnel tested prior to the contract activities. These configurations were shown to have undesirable transonic flow development as a result of the large trailing-edge extensions and inboard airfoil sections.

Thirty-nine wing geometries were examined during the subsequent development of the five test wings – W_3, W_4, W_5, W_7, and W_8. Variations in geometric characteristics included changes in twist distribution and planform as well as in airfoil section definition. Some of the configurations were modified to observe aircraft system constraints.

For the first test wing, W_3, a small inboard leading-edge extension or glove was added to minimize the strength of the inboard shock which had been an unsatisfactory feature of the baseline wing. In addition, the W_3 design introduced a second trailing-edge break to soften the effect of the inboard trailing-edge extension, and modified camber and leading-edge radius on the wing outboard sections.

A later analysis indicated that buffet C_L could be improved with a planform and twist modification designed to lower the local lift coefficients on the outboard wing where flow separation was predicted to start. These changes were used to develop wind tunnel test configuration W_4.

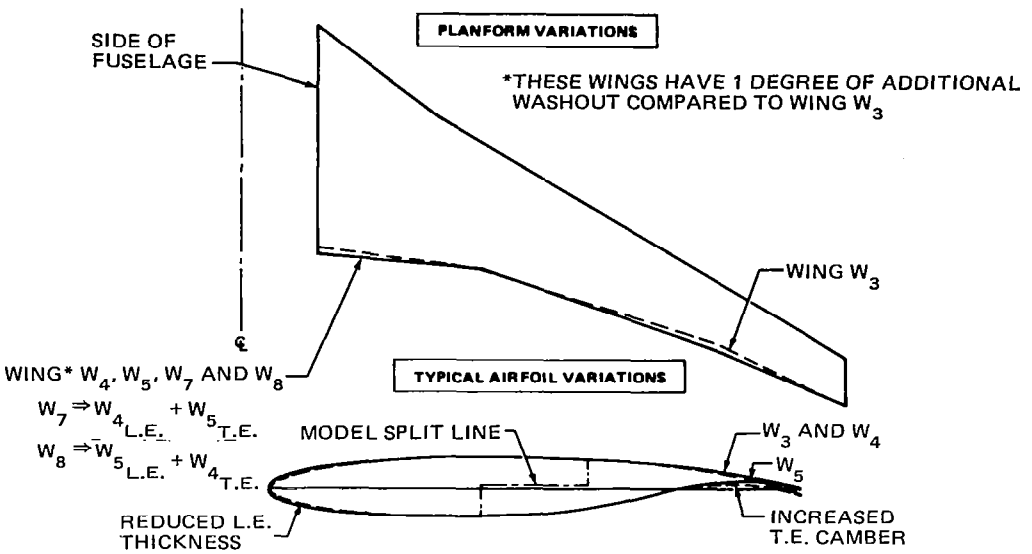

HIGH-SPEED TEST CONFIGURATIONS

Further analysis of the defining airfoils identified areas of potential performance improvement. Reduced leading-edge radius addresses a possible premature drag creep before drag divergence. Increased aft camber improves the buffet C_L provided viscous effects do not cause excessive performance losses. These two variations were used to define test configuration W_5. Models for W_4 and W_5 were built with separate leading and trailing edges. The leading edge of W_4 combined with the trailing edge of W_5 produce model W_7, while the trailing edge of W_4 combined with the leading edge of W_5 produce model W_8. Hence, the effects of the leading-edge and trailing-edge modifications could be evaluated separately as well as together.

Wind Tunnel Models

The 4-percent-scale wind tunnel model series included a fuselage, five wing configurations with accompanying wing-body fillets, tail surfaces, and a set of nacelles, pylons, and flap linkage fairings for one of the wings. Each of the wings was instrumented with static pressure orifices. The models were sting-mounted.

Experimental Program

Four wind tunnel tests were conducted in the NASA Ames Research Center 11-foot transonic wind tunnel. The tunnel provided a range of Mach numbers from 0.5 to 0.925, with Reynolds numbers from 21.3 million per meter to 26.25 million per meter (6.5 million per foot to 8.0 million per foot).

The first test, designated LB-488A, obtained data on wings W_3 and W_4, but suffered from a lack of data repeatability. Most of the test was therefore repeated in the second entry, LB-488C, with much improved reliability. Test LB-488B followed in which four wings (W_4, W_5, W_7, and W_8) were tested. Additionally, wing W_4 was tested with nacelles and pylons, flap linkage fairings, and empennage. The final test, LB-488D, obtained wake pressure profiles and data for wing W_8 to evaluate outboard lateral control devices at cruise and dive Mach numbers.

Results and Evaluation

Basic Data. Drag polar, lift curve, and pitching moment curve data were obtained. Transition-free data were used to define buffet boundary and stability characteristics. Transition-fixed data were used to establish drag-rise characteristics.

Drag Rise. Drag rise data characteristics are shown first without corrections for Reynolds number, for transition location or for differences in the lowspeed due to induced drag.

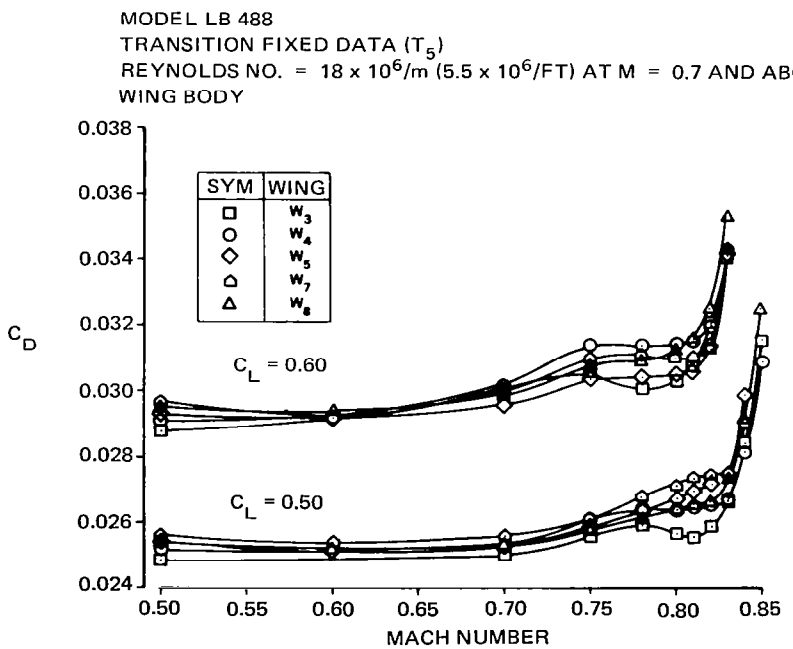

DRAG-RISE CHARACTERISTICS

A more direct comparison of the compressibility drag characteristics can be made with data normalized at M = 0.5. These data are corrected for Reynolds number and transition location.

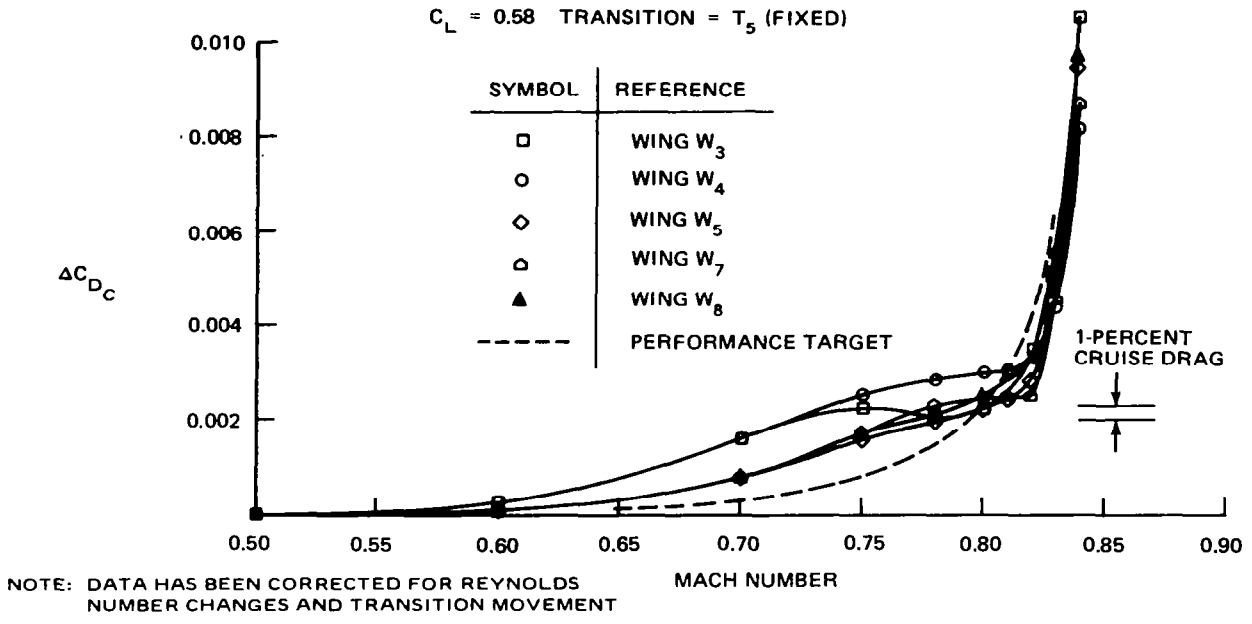

DRAG-RISE CHARACTERISTICS COMPARED

In the Mach number regime between 0.6 and 0.78, the drag creep is the greatest for the wings with the largest nose radii and lowest cambers, W_3 and W_4. Increasing the camber reduces the creep as evidenced by W_5 and W_7, but almost equally as effective is a reduction in the nose radius in combination with the lower camber, W_8. However, since the nose geometry is critical to the development of the supercritical region and since larger radii also benefit the low-speed performance, the amount of nose radius reduction which is practical is limited. Ensuing wake measurements have established that most of the drag creep is due to shock near the leading edge of the inboard wing. Subsequent experimental development work has in fact resulted in the practical elimination of the drag creep.

The drag divergence Mach number, based on $dC_D/dM = 0.05$, was approximately the same for all of the wings tested; only the levels of drag at Mach divergence differ. This Mach divergence of 0.815 to 0.82 was approximately 0.07 to 0.08 higher than that which would be attainable with a conventional wing having the same sweep and thickness; this assumes a lift coefficient of 0.58 and a C_{D_C} of 0.0018 for the conventional wing at Mach divergence.

The compressibility drags at Mach divergence for the wings tested (0.0025 to 0.0035) were higher than those of the conventional wing because of the drag creep. This drag level could be reduced by a reduction in thickness, but tradeoff studies have shown that the weight penalty of the thinner wing has a much greater negative effect on the total airplane than has the increased drag level.

Buffet Boundary. The buffet boundary is one of the most influential aerodynamic characteristics in determining the final wing design. For the high-aspect-ratio wing, the lift coefficient for optimum lift-to-drag ratio is considerably higher than in existing transports. The design task to achieve a good buffet boundary is correspondingly difficult.

A composite curve for all of the wings tested is shown below. It is based primarily on the break in the pitching moment curve, with the lift curve and trailing-edge pressures also used to interpret the data where necessary.

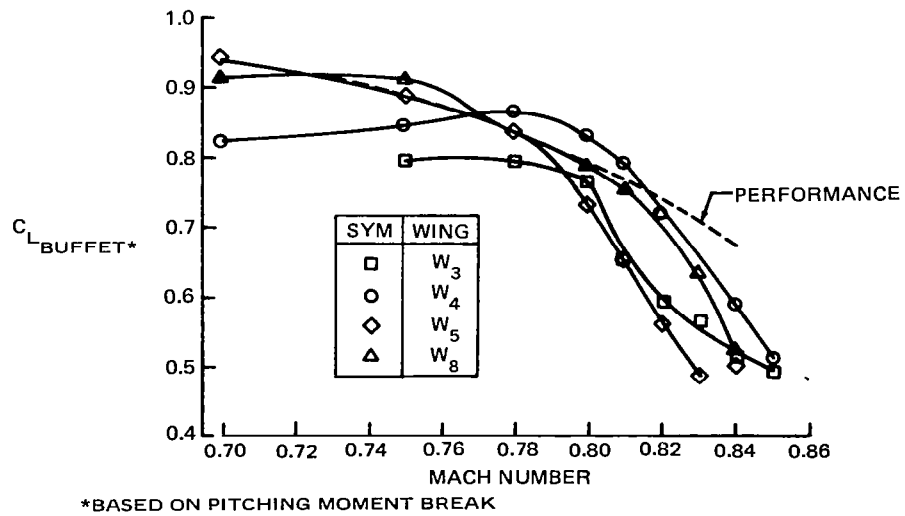

BUFFET BOUNDARIES COMPARED

The results show that it is possible to achieve a buffet boundary consistent with the high cruise-lift coefficient of the high-aspect-ratio supercritical wing. At higher-than-cruise Mach numbers, performance falls short, but requirements in this area have not yet been established.

Interference Effects. The primary effect of interference of the nacelles and pylons alone on the W_4 wing-body lift curve is a loss in lift coefficient at a constant angle of attack of approximately 0.04.

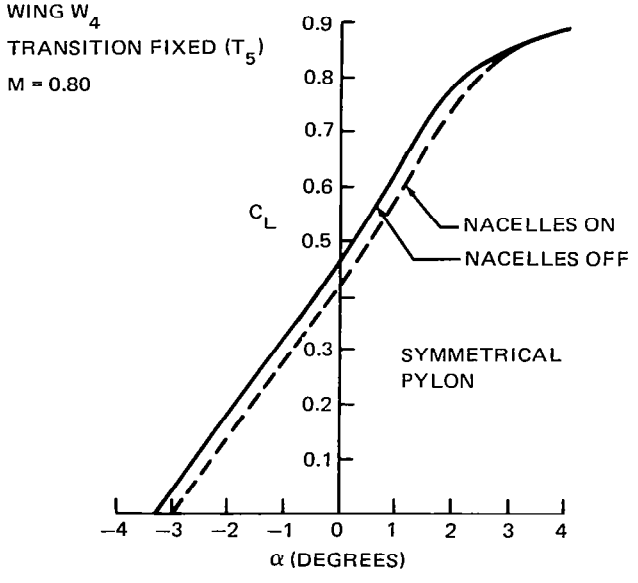

EFFECT OF NACELLES AND PYLONS ON WING-BODY LIFT CURVE

The spanwise distribution of lift was altered by the presence of the nacelles and pylons, as shown for the cruise condition.

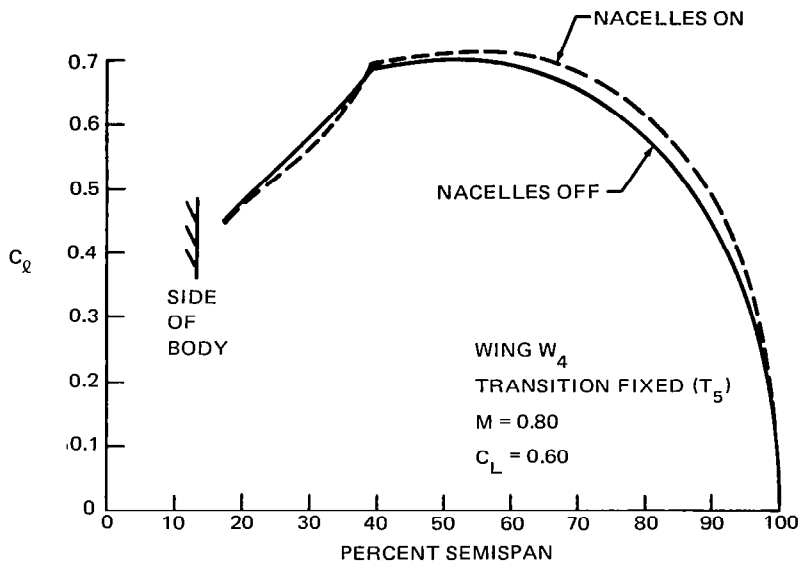

EFFECT OF NACELLES AND PYLONS ON SPANWISE LIFT DISTRIBUTION

Lower wing surface pressure data adjacent to the inboard side of the pylon clearly showed a shock condition, although this effect decayed either side of the pressure row. Based on analytical investigations, the pylon had little effect on the lift at subsonic conditions; the lift loss was almost entirely due to the effect of the nacelle. Therefore, any refinement of the pylon geometry would not be expected to improve the lift loss.

The effect of increasing C_L was found to decrease the excess nacelle/pylon drag increment. This increment became negative at the high-lift coefficients.

The effect of adding flap linkage fairings was to increase the subsonic drag increment but yield a smaller compressibility drag increment.

The nacelles and pylons decreased the drag divergence Mach number. However, the interference of flap linkage fairings regained some of the loss due to the nacelles and pylons.

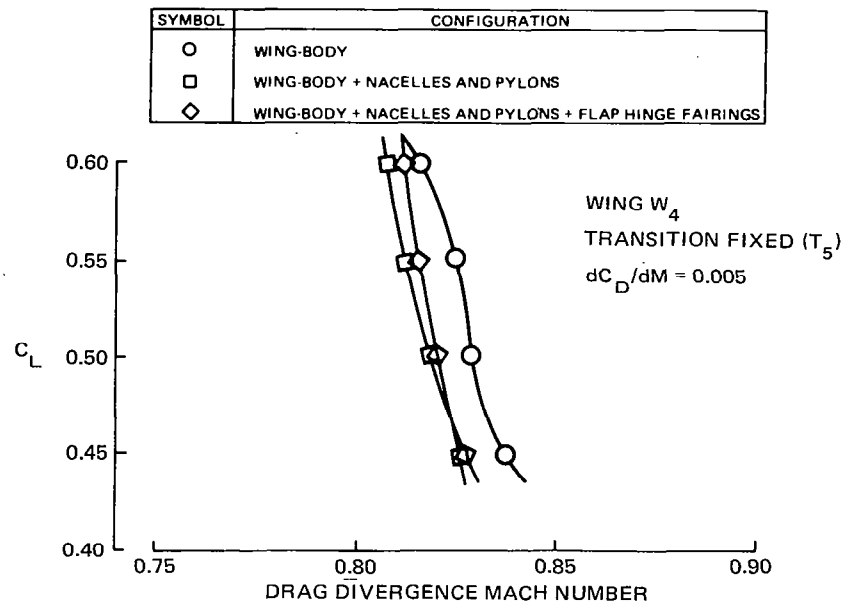

EFFECTS OF NACELLES, PYLONS, AND FLAP LINKAGE FAIRINGS ON DRAG DIVERGENCE MACH NUMBER

The effect of the nacelles and pylons on the wing-body pitching moment at subsonic and cruise Mach numbers was destabilizing. The pitching moment shift at M = 0.8 near zero lift was caused by the aggregation of the change in span loading of the wing, the change in sectional C_m across the span, and the change in C_m due to the angle-of-attack change (fuselage effects) necessary to maintain wing lift coefficient.

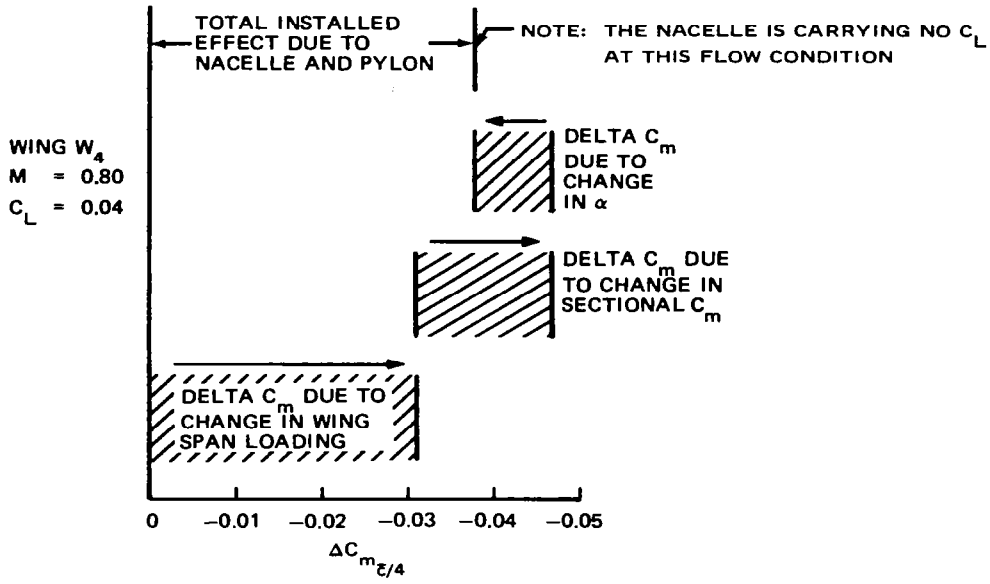

NACELLE AND PYLON INSTALLATION EFFECTS ON THE CONFIGURATION PITCHING MOMENT (TAIL-OFF)

Tail-on Characteristics. Wing W_4 showed acceptable characteristics at high speed (M = 0.80 and above). However, lower-Mach-number data displayed more severe pitchup characteristics due to wing characteristics. This characteristic can be improved by tailoring the loading and airfoil sections.

Trim Drag. Trim drag can be a more significant portion of the total cruise drag of a supercritical wing configuration than a conventional wing due to the higher pitching moment coefficients of the supercritical wing. The increase in trimmed wing C_L for the cruise condition also effectively lowers the buffet boundary. Likewise, the drag divergence Mach number at the trimmed lift coefficient can be lower than that of the simple wing-body configuration.

Furthermore, the relaxed static stability incorporated into the baseline aircraft has the effect of reducing the trim drag relative to a conventionally arranged configuration.

The trim drag for the sting-mounted model at cruise, measured directly from data with the CG at 25 percent of the MAC, was 6.5 percent of total cruise drag. Correction for the sting effect on downwash resulted in a 3.5-percent reduction. At the midpoint of the configuration CG range at 19-percent MAC, the trim drag was increased for a total of 4.8 percent of total cruise drag. It is apparent that the trim drag of the wide-body supercritical wing configuration was a significant portion of total cruise drag, an order of magnitude larger than that of the conventional-winged DC-10.

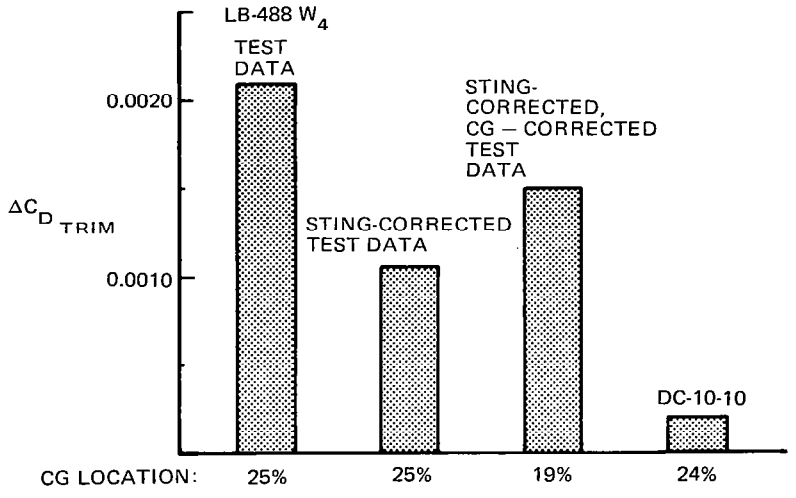

CRUISE TRIM DRAG

Wake Rake Results. Wake measurements were obtained for wing configuration W_8 using the Douglas traversing wake rake. The measured wake profiles were integrated to obtain section profile drag. At M = 0.75, a region of concern because of drag creep, the inboard wing near 30-percent semispan was shown to contribute the most to the creep. By the time the drag divergence Mach number, 0.82, was reached, strong shocks had developed on both the inboard and outboard wing. Spanwise distributions of section profile drag were integrated to obtain the total wing profile drag.

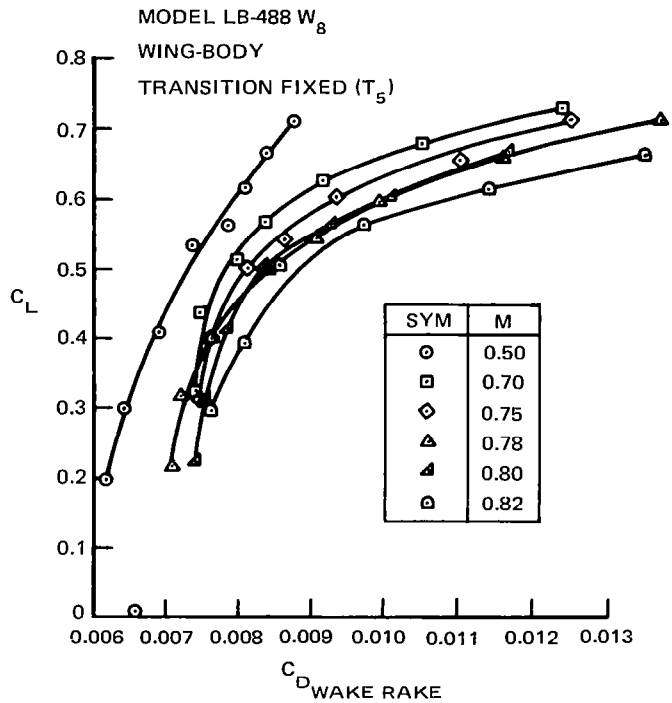

WAKE RAKE WING PROFILE DRAG POLARS

Compressibility drag increments obtained from the wake rake measurements agreed well with those obtained from the force balance measurements.

In addition to the T_5 transition configuration, an alternate transition configuration near the leading edge, T_6, was also tested to compare the effect on integrated profile drag at M = 0.5. The steep curve with transition forward results from a lack of pressure recovery near the trailing edge at the lower lift coefficients. Using the aft transition location, sublimation studies showed that natural transition was occurring forward of the upper surface trip at the higher lift coefficient, so this curve is not truly representative either. If higher Reynolds number flow could be properly simulated, the resulting profile drag polar would be somewhere between these two limits.

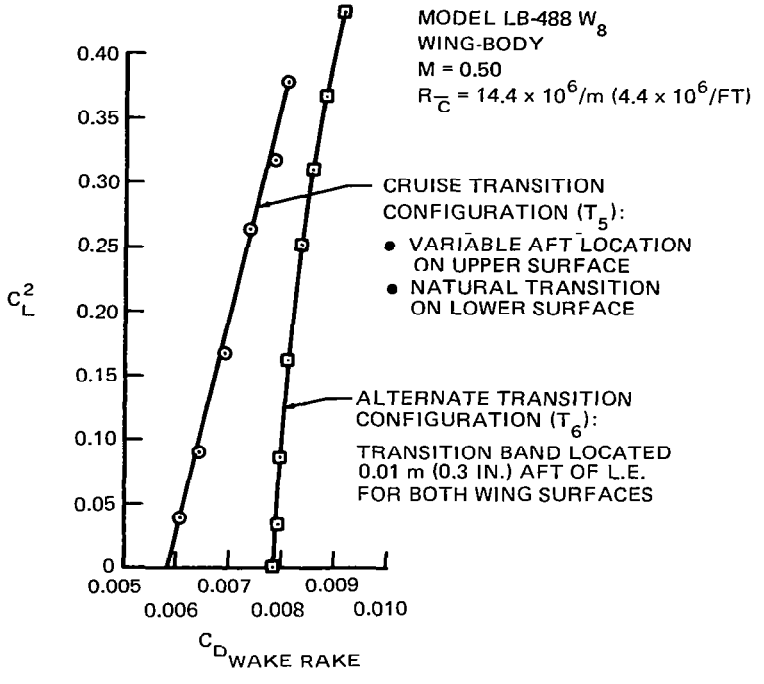

EFFECT OF TRANSITION CONFIGURATION ON WING PROFILE DRAG POLARS

Aileron Effectiveness. Data obtained in the fourth test of the series, LB-488D, included testing of an outboard aileron at high Mach numbers. This aileron, installed in the right wing, showed that aileron effectiveness was acceptable within the wing dive Mach number limit of 0.90.

HIGH-ASPECT-RATIO SUPERCRITICAL WING HIGH-LIFT DEVELOPMENT*

Objective

The objective of this task was to develop the high-lift technology for the high-aspect-ratio supercritical wing.

Approach

Using two- and three-dimensional analytical methods, leading- and trailing-edge devices for the baseline were designed to meet landing and takeoff requirements. These designs were verified in wind tunnel model tests, and correlations were made with predictions.

Preliminary Trade Studies

Studies were conducted comparing the baseline aircraft having a high-aspect-ratio supercritical wing with an equivalent having a currently conventional wing. Significant performance benefits accrue to the aircraft with the advanced wing.

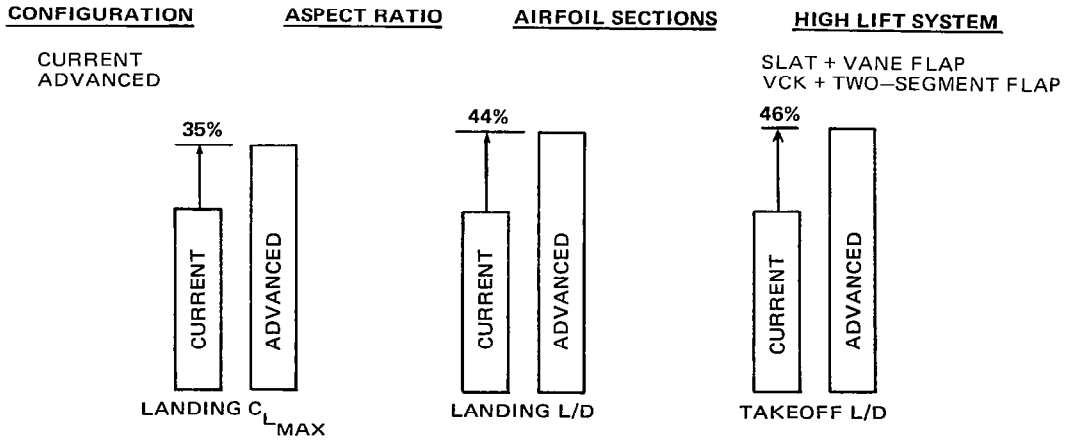

COMPARISON OF LOW-SPEED CHARACTERISTICS FOR CURRENT AND ADVANCED TRANSPORTS

*The contract work is reported in detail in the document of Reference 2.

An additional study compared the effect of conventional and advanced high-lift systems applied to the high-aspect-ratio supercritical wing. A substantial gain resulted due to the VCK, two-segment flap and flaperon. As in the first trade study, the improvement in landing L/D would result in a substantial reduction in approach noise.

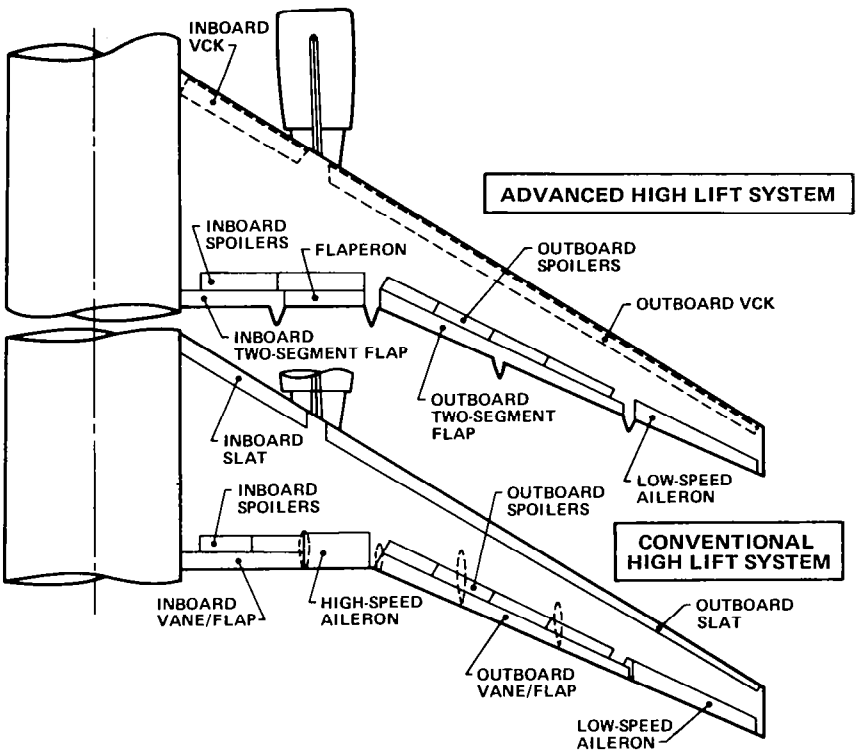

ADVANCED AND CONVENTIONAL HIGH LIFT SYSTEMS

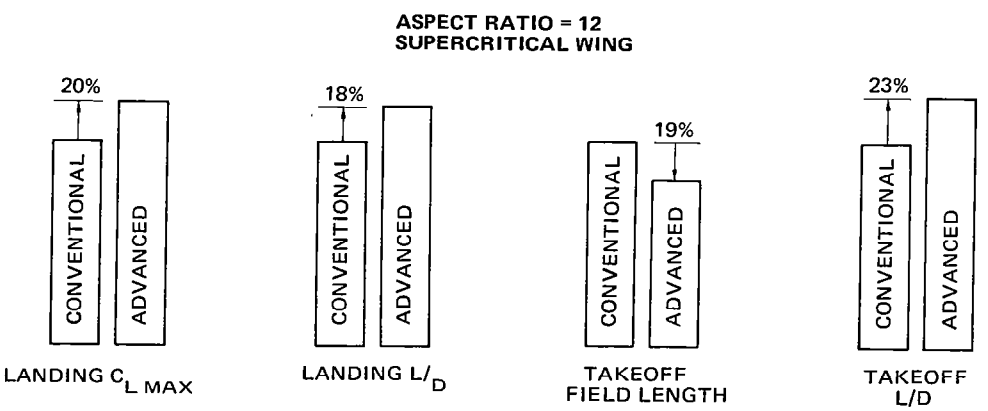

PERFORMANCE OF CONVENTIONAL AND ADVANCED SYSTEMS

Design of High-Lift Devices

With the high-lift concepts selected and the guidelines for the related structural constraints defined by the results of in-house studies, the high-lift systems were designed for the wind tunnel model. The design function consists of four basic parts — the experimental data base, two-dimensional analytical studies, modification of data from two-dimensional to three-dimensional, and the three-dimensional lifting surface calculations.

Wind Tunnel Model

The wind tunnel model was a 4.7-percent scale representation of the baseline aircraft.

The model wing incorporated:

- A cruise leading edge, removable at the front spar and able to simulate VCK stowage wells. Also provided was a WUSS leading edge for the slat configuration.
- A VCK and slat leading-edge device with variable position and deflection capability.
- A two-segment trailing-edge flap supported at five deflection angles by fixed brackets simulating the airplane flap linkage. Variable position capability was provided for the main flap.
- A manually set aileron, left side only, and spoilers, both sides.
- Approximately 400 static-pressure orifices installed in the VCK, slat, wing, and flaps.

Experimental Program

The first test (LB-486A) was conducted at the NASA Ames Research Center in the 12-foot pressure wind tunnel. Data for various Mach and Reynolds numbers were obtained. A majority of the configurations were evaluated at high Reynolds number. The normal test condition developed a Reynolds number of 20 million per meter (6 million per foot) at 0.2 Mach number.

The first test evaluated aerodynamic characteristics for:

- Basic clean wing
- Leading-edge-device optimization
- Two- and single-segment flap optimization
- Nacelle/pylon and landing gear effects
- Effect of inboard VCK and slat span
- Horizontal tail-on characteristics for selected configurations
- Clean trailing-edge characteristics
- Clean leading-edge characteristics
- VCK well effects
- Aileron evaluation with high-lift system
- Effect of minitufts on high-lift characteristics

The second test (LB-486C) was conducted at the NASA Langley Research Center in the V/STOL wind tunnel. Spoiler configurations were included. The normal test condition developed Reynolds numbers of 4.5 million per meter (1.4 million per foot) at 0.2 Mach number.

Results and Evaluation

Basic Clean Wing. The clean wing achieved a high level of $C_{L_{MAX}}$ (1.513) and L/D at 1.2 V_S (19.45)

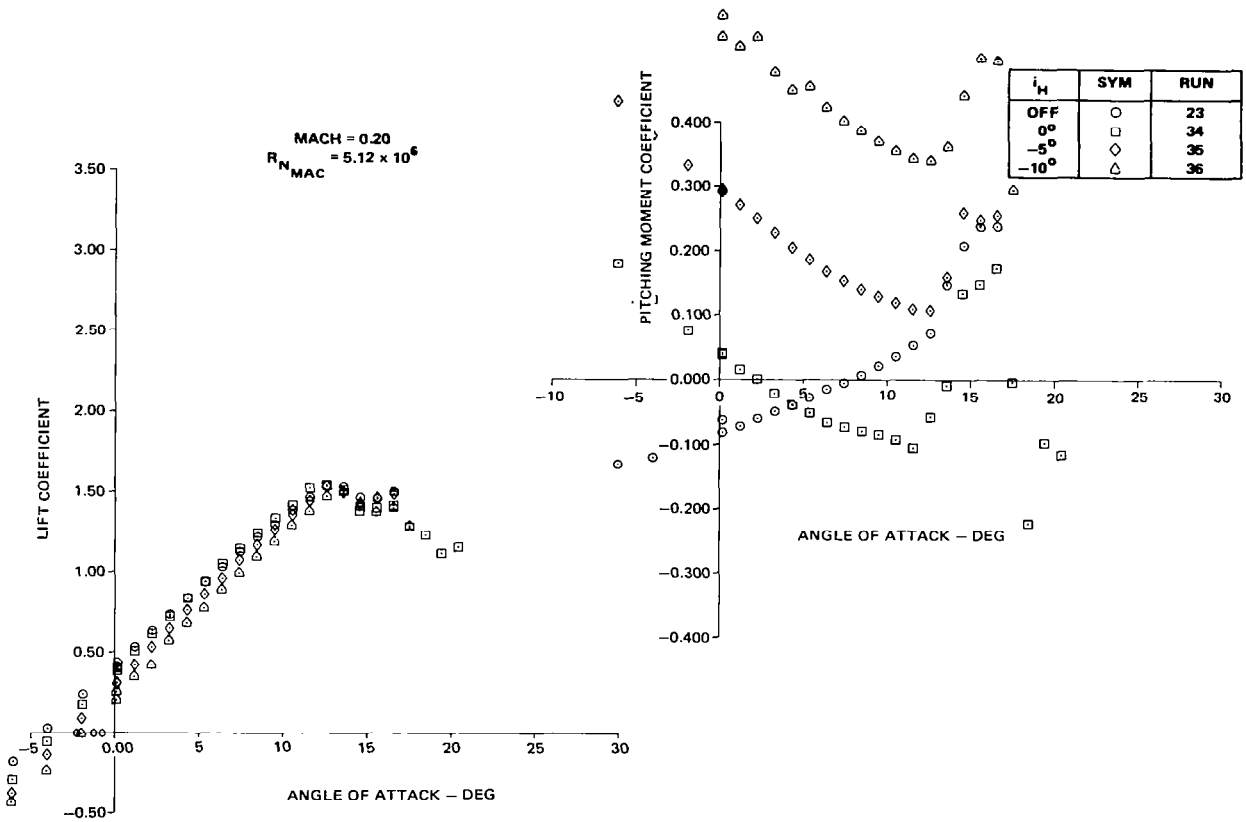

TAIL-ON CHARACTERISTICS FOR THE CRUISE WING – LIFT AND PITCHING MOMENT

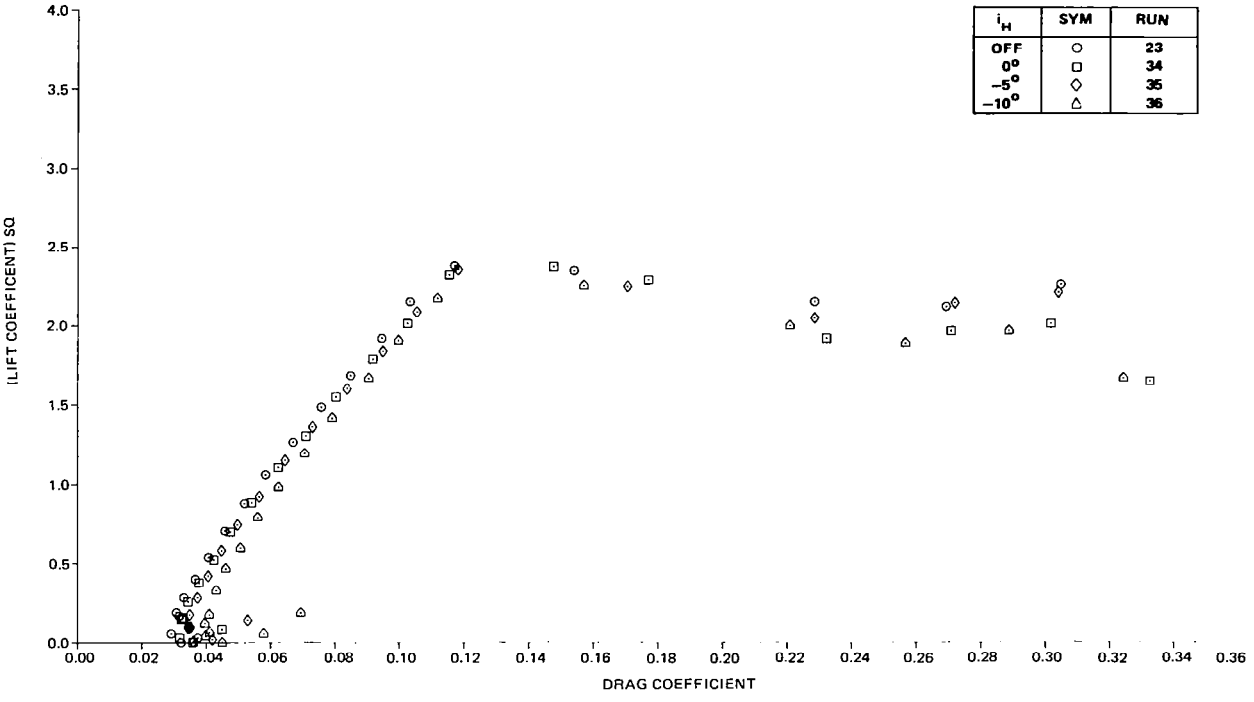

TAIL-ON CHARACTERISTICS FOR THE CRUISE WING – DRAG COEFFICIENT

Addition of the nacelles, pylons, and strakes resulted in a negligible change in $C_{L_{MAX}}$, a reduced L/D (17.7), and improved pitch characteristics at high angles of attack. Increasing the Reynolds number from atmospheric to the high Reynolds number test condition increased the $C_{L_{MAX}}$ significantly ($\Delta C_{L_{MAX}} = 0.39$). A Mach number increase from 0.20 to 0.32 resulted in a decrease in $C_{L_{MAX}}$ of 0.11. Test data for the cruise wing configuration with the horizontal tail indicated the low-speed pitch characteristics require improvement. It should be noted that the ongoing high-speed wing development for the family of configurations has altered the span loading in a direction to improve the low-speed stalling behavior.

After correction of the experimental data for wind tunnel wall effects and the influence of the model support system, good agreement with theoretical prediction was found for the lift and section pressure cases examined. Comparisons of spanwise variation of sectional lift coefficient data with prediction showed good agreement inboard, but some overstatement of outboard values in the prediction.

Slat and VCK Leading-Edge-Device Optimization. The slat was superior to the VCK in $C_{L_{MAX}}$ and L/D performance. However, pitch characteristics were superior with the VCK. VCK data indicated that improved performance may be achieved by reducing its deflection. The superior VCK pitch characteristics resulted from an increased amount of inboard stall relative to the slat configuration, and the ability of the VCK to prevent significant lift loss over the outboard wing. The VCK cutout at the nacelle pylon and the fuselage side contributed to the improvements inboard. The best compromise between performance and stability and control for the VCK was obtained with a 45-degree VCK deflection. For the slat, this relationship was best with deflections of 15 degrees inboard and 25 degrees outboard. Improvements both in aerodynamic performance and pitch could result from further leading-edge-device optimization.

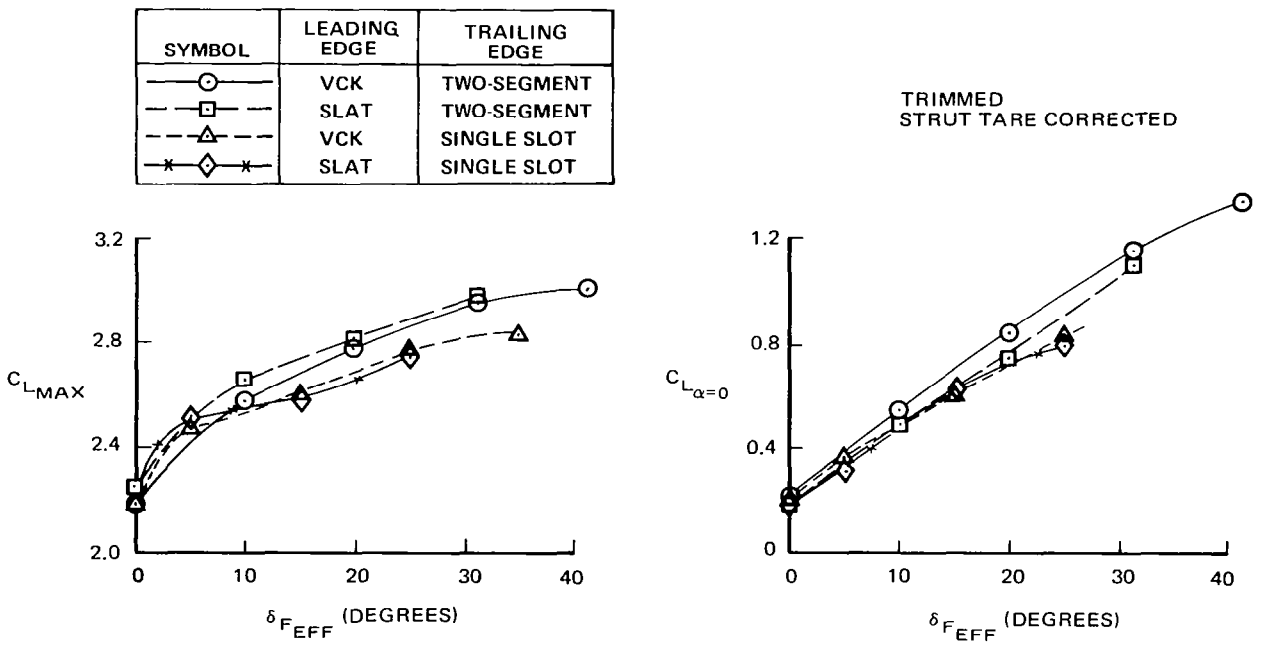

EFFECT OF LEADING AND TRAILING EDGE HIGH-LIFT CONFIGURATION ON $C_{L_{MAX}}$ AND $C_{L_{\alpha=0}}$

Two- and Single-Segment Flap Optimization. Trailing-edge flap investigations indicated that changes in performance due to gap and overhang variations of the flap system were not as significant as the corresponding variations for the leading-edge devices. Flap optimization was investigated with the VCK only.

From the standpoint of $C_{L_{MAX}}$, L/D at 1.3 V_S, and pitching moment characteristics, the following two-segment configurations were chosen as the best:

Main flap	Second Segment
35 degrees	12 degrees (limited data only)
25 degrees	12 degrees
15 degrees	10 degrees
5 degrees	10 degrees

Similarly, with the single-slot flap, little change occurred in characteristics with the changes in the configuration. As the flap deflection was reduced, more favorable pitch characteristics after $C_{L_{MAX}}$ were obtained. Main flap positions selected were 25, 15, and 5 degrees.

Nacelle/Pylon Effects with VCK. Addition of the nacelles, pylons, and strakes for the landing flap deflection resulted in a positive increment in pitching moment and a small reduction in $C_{L_{MAX}}$. The pitch trends at angles of attack greater than 22 degrees are similar, but at a different level. Removal of the over-the-pylon-VCK extension resulted in a further reduction in $C_{L_{MAX}}$ but improved high angle-of-attack pitch characteristics.

Landing Gear Effects. The C_D increment due to the landing gear is approximately 0.25 at zero lift, reducing slightly with increasing C_L values. The increment for takeoff or landing flap deflections is similar. The effect of the landing gear on $C_{L_{MAX}}$ is negligible for takeoff flap and -0.076 for the landing flap.

Effect of Inboard VCK and Slat Span. The full-span VCK, without nacelles and pylons, achieved a $C_{L_{MAX}}$ of 3.4 with landing two-segment flap deflections. This $C_{L_{MAX}}$ reduced to 3.2 with the normal VCK cutouts. However, the pitch characteristics were improved. The slat configuration was sealed in the area of the pylon and had an inboard trim position closer to the fuselage side. Improved pitch trends could result from increased outboard trim position (further from the fuselage and nearer the VCK spanwise position), and a revised trim over the pylon.

The slat-extended flaps-retracted pitching moment variations were improved significantly by a revised trim position for the inboard slat. This revised position was at an increased distance from the fuselage side. Future development of the flaps-deflected case at high Reynolds number is expected to improve the pitching moment further.

Horizontal Tail-on Characteristics. The tail provided nose-down pitching moment with the VCK and two-segment flap near $C_{L_{MAX}}$ for −15 and −5-degree settings. The zero-degree setting provided close-to-zero pitching moment near $C_{L_{MAX}}$. The character of the pitching moment was not altered by Reynolds number. With the single-slot flap also, pitching characteristics were affected similarly.

With the slat, the tail-on stability was unsatisfactorily reduced prior to $C_{L_{MAX}}$. Further development, including modifications to increase lift loss inboard, is necessary with this configuration.

Clean Leading Edge. Results with a clean leading edge showed that the development of the leading-edge configuration was of equivalent importance to the development of the trailing edge. Without the leading-edge device (clean leading-edge configuration), the $\Delta C_{L_{MAX}}$ with flap deflection was only 0.6. Achievement of large $C_{L_{MAX}}$ for these configurations requires significant leading-edge protection for the outboard wing panel.

Clean Trailing Edge. The slat-extended flaps-retracted pitching moment variation was improved significantly by a revised trim position for the inboard slat. This revised position was at an increased distance from the fuselage side.

VCK Wall Effects. Only minor effects were encountered due to the opening of VCK walls to airflow.

Aileron and Spoiler. At pre-stall angles of attack, the aileron effectiveness is well-behaved for the clean and landing configurations. The takeoff configuration data exhibit similar trends except near the stall where the effectiveness of the downgoing aileron is diminished. Trailing-edge-up deflections were much more effective (in some cases, twice) than trailing-edge-down deflections.

The spoiler data indicate well-behaved characteristics for the three configurations with increasing effectiveness being shown for increased flap deflections.

Effect of Minitufts on High Lift Characteristics. Both with the clean wing and with high lift devices deployed, the effect of minitufts was very small on lift pitching moment and slight on drag.

Performance Summary. The following figures summarize the performance characteristics and show correlations with theoretical methods. Theoretical results were calculated by the Giesing vortex lattice method and the Douglas version of the Jameson-Caughey (FL022) three-dimensional transonic flow program.

Clean wing basic data show corrections for wind tunnel wall effects. The flagged symbols have further corrections for the influence of the model support system. The fully corrected data agree well with prediction. Good agreement is also shown with wing pressure comparisons.

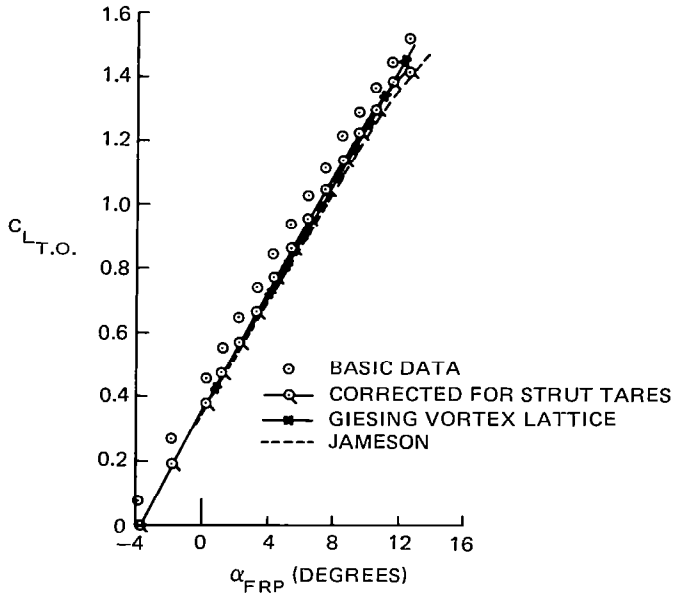

LIFT COMPARISON FOR CRUISE WING

As expected, the two-segment flap was superior to $C_{L_{MAX}}$ and flap lift increments. Trimmed polar comparisons indicated equivalent L/D envelopes for takeoff flap settings.

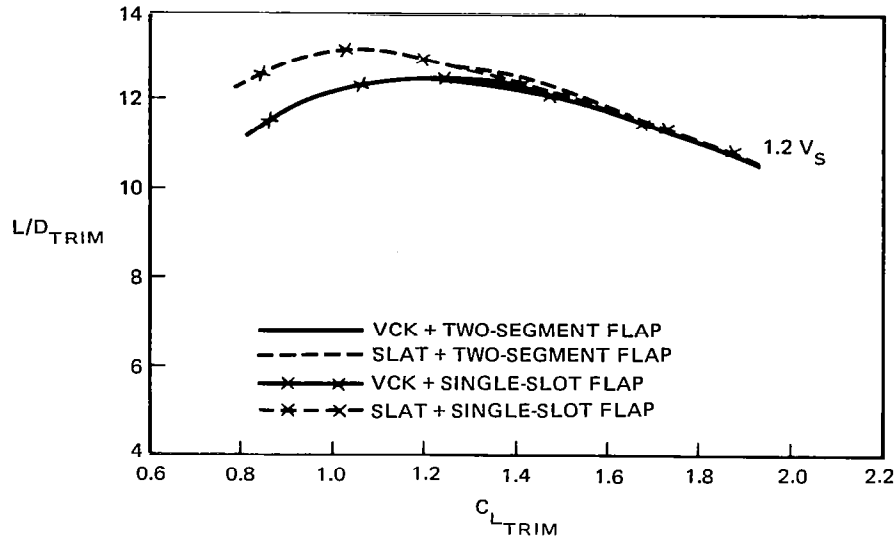

TRIMMED L/D COMPARISON FOR THE TAKEOFF CONFIGURATION

For equivalent values of approach speed, the L/D values for the two-segment flap were superior to the single slotted flap. Improvement of pitch characteristics may be obtained in the future by means of different flap deflection for the inboard and outboard sections.

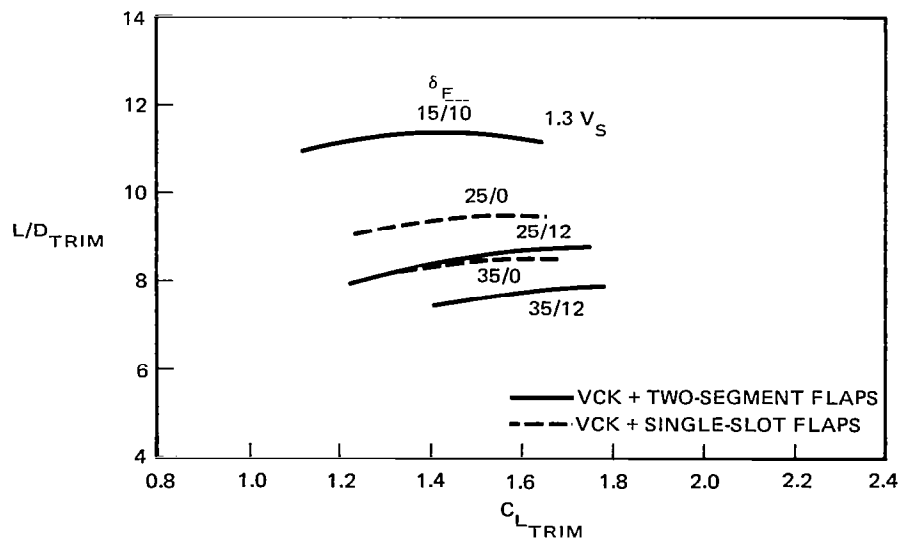

TRIMMED L/D COMPARISON BETWEEN TWO-SEGMENT AND SINGLE-SLOT FLAPS FOR THE LANDING CONFIGURATION

Good agreement was shown in the results providing maximum lift increments for the VCK and the two-segment flap system.

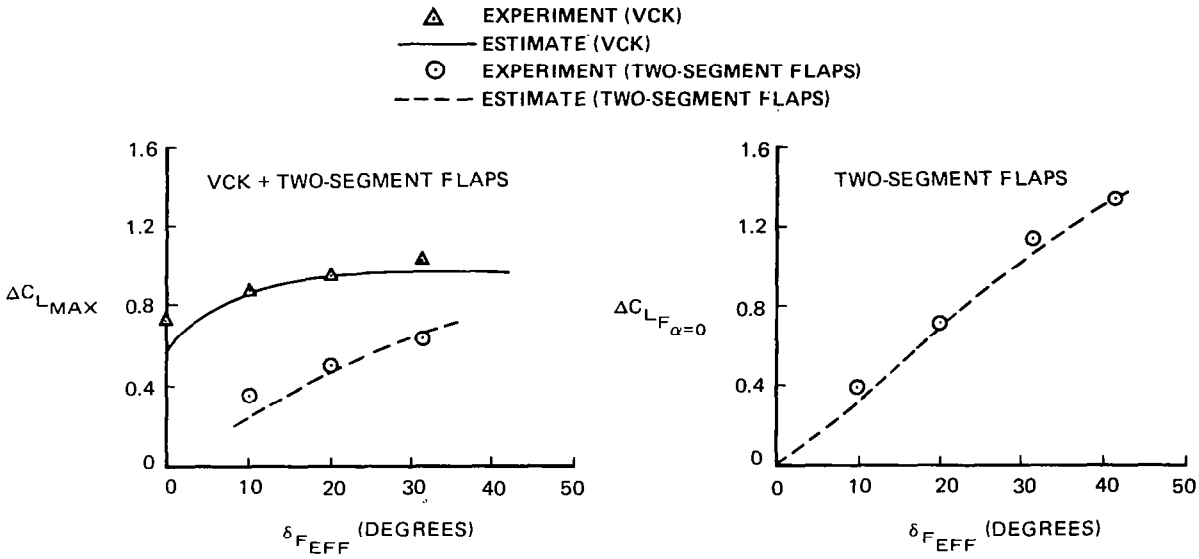

COMPARISON OF EXPERIMENTAL AND ESTIMATED MAXIMUM-LIFT INCREMENTS FOR VCK AND FLAPS, AND FLAP-LIFT INCREMENT AT ZERO ANGLE OF ATTACK

The trimmed $C_{L_{MAX}}$ comparison indicated good agreement at zero and maximum flap deflections. For the takeoff flap deflections, the estimated $C_{L_{MAX}}$ values were lower than the experimental data. The estimates were, in general, conservative for the VCK with two-segment flap configuration.

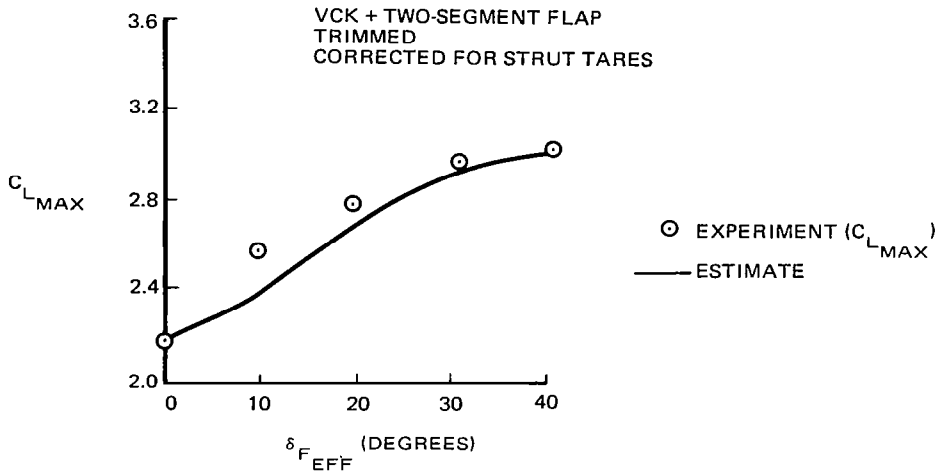

COMPARISON OF ESTIMATED AND EXPERIMENTAL $C_{L_{MAX}}$

Comparison of tail-off L/D data for the VCK with two-segment flap configuration is shown here. Agreement is good.

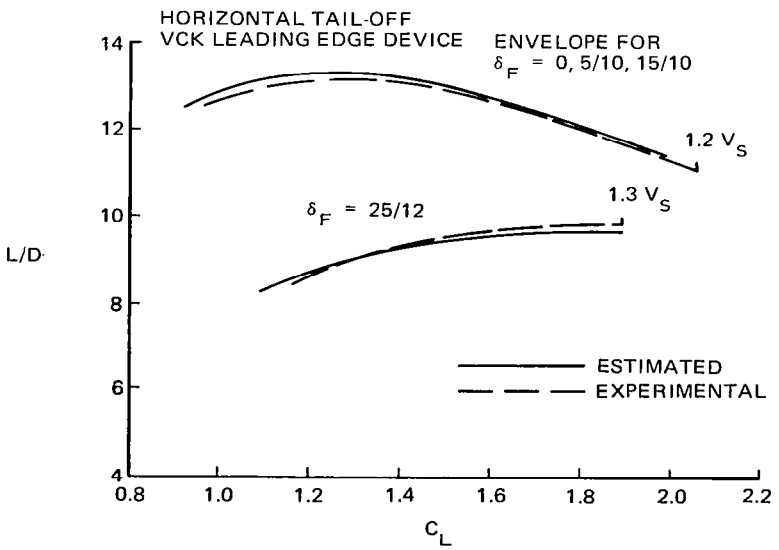

COMPARISON OF EXPERIMENTAL AND ESTIMATED L/D CHARACTERISTICS

STUDY OF A TRANSPORT CONFIGURATION WITH SUPERCRITICAL WING AND WINGLET*

Objective

The objective was to compare an advanced commercial transport with a wing-winglet (designed in combination from the outset) with the baseline aircraft.

Approach

A series of wing-winglet combinations for the baseline mission requirements were designed. The aerodynamic characteristics of each configuration were constrained to the values for the baseline, and the "optimum" wing-winglet was the one chosen solely on the basis of minimum structural weight. After selection of the lightest winglet, the aircraft configuration was refined by a resizing process, and its weight and performance recalculated. Direct operating costs were estimated and compared with the baseline.

Selection of Wing-Winglet Configuration

Wing Design Rules. In order to match the most important performance characteristics of the baseline, each wing-winglet design obeyed the following rules:

- The induced-drag coefficient should match the baseline value.
- The trapezoidal wing area, leading-edge sweep, and trailing-edge sweep should match the baseline value. The baseline airfoil section at the aerodynamic definition points should be identically employed. In addition, the geometry of the inboard trailing edge should make proper provision for the retracted main landing gear.
- The wing dihedral angle should match the baseline value.

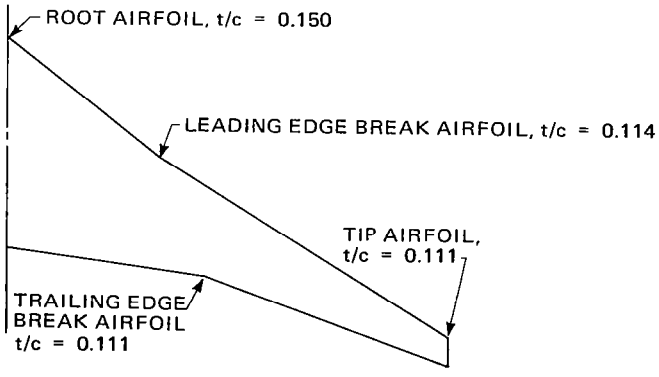

AIRFOIL DEFINITION FOR WING-WINGLET CONFIGURATION

*The contract work is reported in detail in the document of Reference 3.

Winglet Design Rules. The winglet was designed to the same general parameters as that wind tunnel tested for the DC-10 Series 30 (Reference 4). This design adhered closely to the original NASA recommendations for the winglet concept. The study included the upper-surface winglet only. From the test results referred to, the lower winglet should produce an additional benefit, and therefore the study results are deemed conservative in this regard. The winglet span for all the configurations generated was 14.8 percent of the wing semispan. An illustration of one of the winglet configurations is shown below.

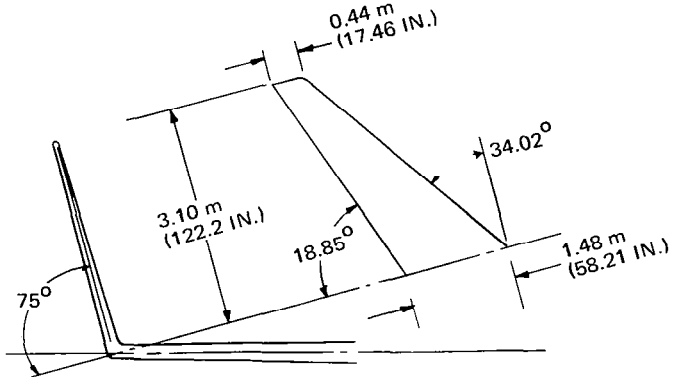

SAMPLE WINGLET PLANFORM FOR WING-WINGLET COMBINATION

Wing-Winglet Planform. The wing and winglet design rules completely specified a configuration except for the most significant parameter, wing span. Maintaining constant induced drag at a specified lift while varying the configuration wing span required a variety of spanwise load distributions among the competing designs. A minimum span exists for a wing-winglet combination beyond which the required induced drag cannot be maintained. At this minimum span, the wing-winglet combination is loaded for its minimum induced drag. At spans greater than the minimum value, the spanwise load distribution may be altered from that for minimum induced drag in a manner that is advantageous from a structural viewpoint.

The relationship between aerodynamic induced drag and structural impact may be indicated simply by comparing drag efficiency factor with wing root bending moment. The wing root bending moment is an indicator of wing weight. The drag efficiency factor is a simple way of expressing the level of inviscid-induced drag relative to the minimum for a

given lift system. For a conventional wing, theory predicts that the factor has a maximum value of one; for a wing-winglet, the factor is predicted to be higher than one. Four alternative wing-winglet design planforms — WW2, WW4, WW5, and WW7 — are compared here with the isolated conventional wing.

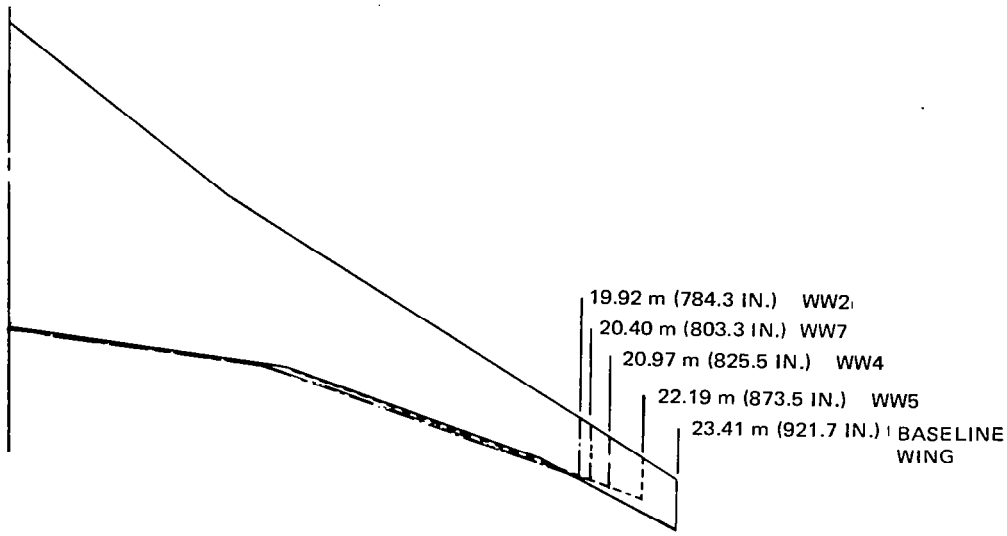

PLANFORMS FOR WING-WINGLET OPTIMIZATION

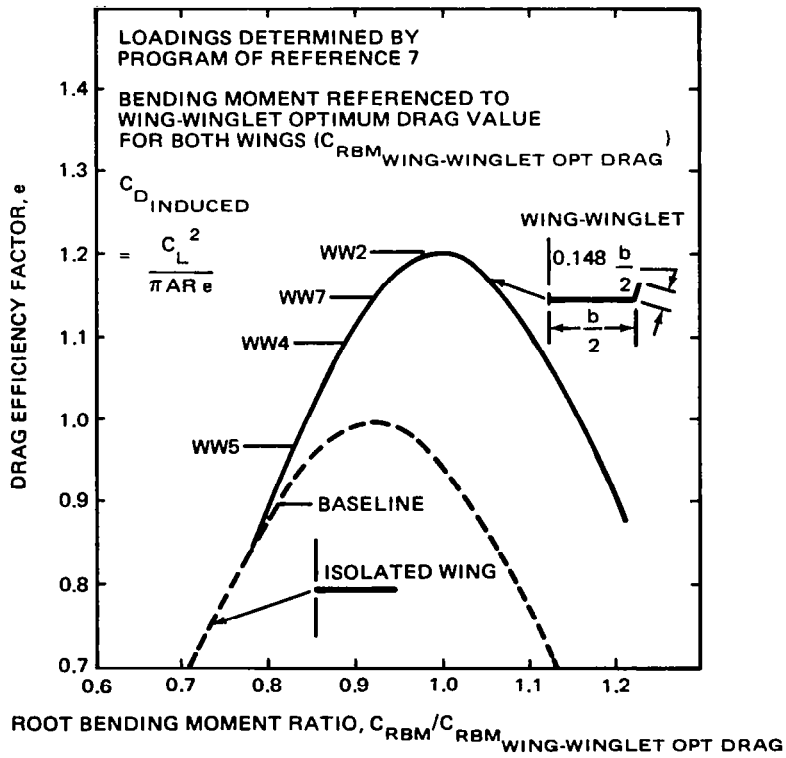

MINIMUM INDUCED DRAG FOR SPECIFIED ROOT BENDING MOMENT

Aerodynamic Analysis. During more refined analysis of spanwise wing loading, the outboard section lift coefficients of WW2 were found to be unacceptable from the viewpoint of buffet and consequently this configuration was eliminated.

The study then derived the required twist distribution in order to obtain the desired wing and winglet loadings. The candidate configurations were then analyzed to verify the design-induced drag value and derive aerodynamic loads for structural design.

Structural Analysis. Each wing-winglet configuration structure was initially sized for ultimate strength requirements and then adjusted as necessary to meet the predicted flutter requirements.

All configurations were subjected to the criteria of FAR Part 25, Airworthiness Standards for Transport Category Airplanes. Critical maneuver and gust conditions were investigated. The winglet and tip portions of the wing for winglet configurations were determined to be lateral-gust-critical; the wing was determined to be maneuver-critical. The flutter analysis idealization represented the fuselage, wing, winglet, and engine pylon flexibility but the empennage was considered to be rigid. Only symmetric flutter modes were analyzed since, for the types of configurations under study, asymmetric modes are not critical. Unsteady aerodynamic influence coefficients were calculated. All aerodynamic coupling among the fuselage, wing, winglet, nacelle, pylon, and horizontal stabilizer was modeled. The theoretical coefficients were weighted to reflect available estimated study aerodynamic data from wind tunnel tests of comparable configurations.

Two flutter modes existed for each wing-winglet configuration. The lower-frequency mode was the basic wing inner panel bending/torsion mode evident even without the presence of the winglet. For low-fuel conditions, this mode was of the "mild humping" type (damping decreases gradually as airspeed increases). The WW7 configuration met the requirement of a flutter speed in excess of 1.2 times the dive-speed mode while the other two configurations (WW4 and WW5) did not.

In addition, a higher frequency outer wing torsion mode was predicted for each of the wing-winglet configurations. The mode was introduced by the large vertical displacement between the winglet center of mass and the wing plane. As a result, the flutter speed was very sensitive to wing span. The predicted flutter speed for this mode was below the requirement only for configuration WW5.

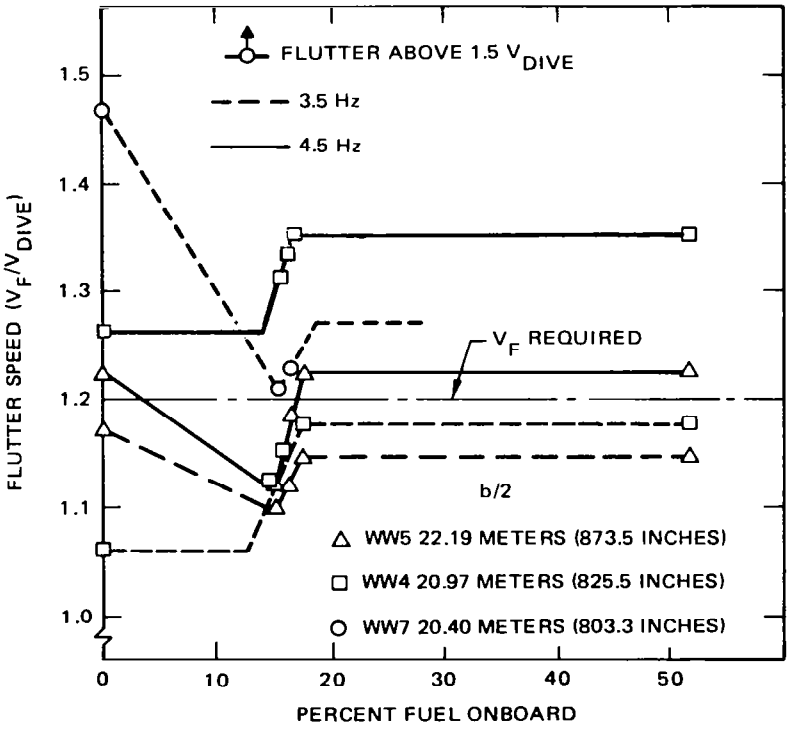

WING-WINGLET CONFIGURATION CHARACTERISTICS

Configuration Data. From detailed studies of the configurations, the elements affecting the weight were established. These elements are identified in the following two figures. Wing bending material weight was lower for the wing-winglet designs, and the weight associated with meeting the flutter requirement was clearly more important for some candidates.

		WING		WINGLET		CONFIGURATION WEIGHT kg (LB)		CONFIGURATION WEIGHT RELATIVE TO BASELINE kg (LB)		
CONFIGURATION	EFFICIENCY FACTOR, e	SEMISPAN, m (IN.)	ASPECT RATIO	SPAN, m (IN.)	ROOT CHORD, m (IN.)	BENDING MATERIAL	FLUTTER PENALTY	BENDING MATERIAL	BENDING MATERIAL WINGLET AND MISC	TOTAL (INCLUDING FLUTTER REQUIREMENTS
BASELINE	0.90	23.41 (921.7)	10.85	–	–	8,100 (17,858)	0	–	–	–
WW5	0.97	22.19 (873.5)	9.73	3.284 (129.3)	1.15 (45.1)	7,731 (17,044)	>318 (>700)	−369 (−814)	−260 (−573)	>58 (>127)
WW4	1.09	20.97 (825.5)	8.70	3.104 (122.2)	1.48 (58.2)	7,413 (16,342)	318 (700)	−688 (−1516)	−545 (−1201)	−227 (−501)
WW7	1.15	20.40 (803.3)	8.24	3.020 (118.9)	1.64 (64.6)	7,362 (16,230)	0	−738 (−1628)	−562 (−1240)	−562 (−1240)
WW2	1.21	19.92 (784.3)	7.86	2.949 (116.1)	1.79 (70.4)	7,496 (16,526)	UNKNOWN	−604 (−1332)	−420 (−925)	UNKNOWN

WING-WINGLET CONFIGURATION CHARACTERISTICS

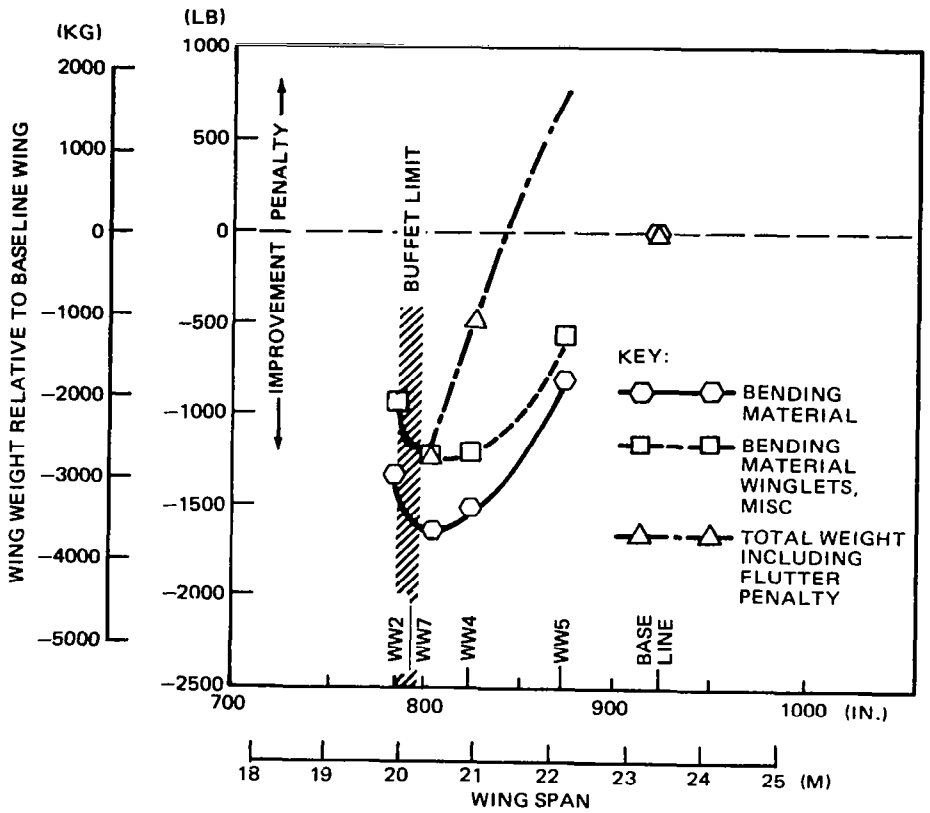

CONFIGURATION WEIGHT INCREMENTS

The shortest-span configuration which satisfied a simple buffet requirement (WW7) was also the lightest wing-winglet design. Therefore, this configuration was selected for the refining configuration design and sizing, and the final evaluation.

This aircraft configuration was based on combination WW7.

CHARACTERISTICS DATA			
ITEM	WING	HORIZONTAL TAIL	VERTICAL TAIL
AREA, SQ m (SQ FT)	202.1 (2175)	56.7 (610)	37.6 (405)
ASPECT RATIO	8.24	3.8	1.6
TAPER RATIO	0.27	0.35	0.35
SWEEP, c/4	30^{o}	30^{o}	35^{o}
DIHEDRAL, c/4	4^{o}	10^{o}	–

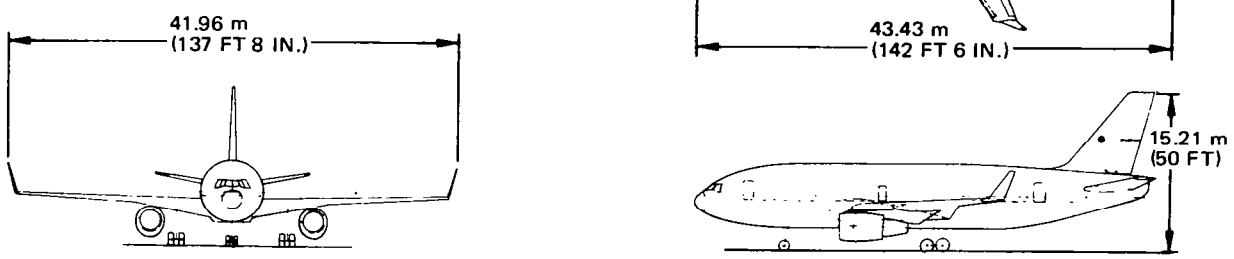

SELECTED WING-WINGLET CONFIGURATION

Refined Configuration Design and Sizing. Following selection of the wing-winglet combination, detailed aerodynamic characteristics were estimated to facilitate sizing-performance calculations. The aircraft was then resized and performance estimated for a typical mission.

As previously mentioned, the wing-winglet configuration was designed to match the baseline-induced drag at the design lift coefficient (C_L = 0.60). However, the induced drag differed slightly from the baseline values at off-design lift coefficients. A reduction in wing-winglet tail compressibility drag, relative to the baseline value, was estimated as a result of the smaller wing-winglet size.

The high-lift characteristics of the wing-winglet configuration were estimated to be slightly degraded compared with those of the higher-aspect-ratio baseline design. The combination had a smaller flapped-wing area. A slightly degraded lift-to-drag ratio resulted from an assessed inability of the winglet to reduce the induced drag of the flap-dominated configuration as effectively as for the cruise configuration.

The aircraft was optimally resized by determining the takeoff gross weight and wing area needed to meet approach speed and initial cruise altitude requirements for the specified design range and payload. The wing-winglet aircraft had a larger wing area but was lighter than the baseline.

	BASELINE AIRCRAFT	WING-WINGLET CONFIGURATION
SIZING RESULTS		
MAXIMUM TAKEOFF GROSS WEIGHT	133,825 kg (295,035 LB)	132,473 kg (292,055 LB)
OPERATING EMPTY WEIGHT	79,255 kg (174,728 LB)	78,573 kg (173,270 LB)
OPERATIONAL LANDING WEIGHT	106,032 kg (233,762 LB)	105,283 kg (232,111 LB)
LANDING FLAPS	20/10 DEG	20/10 DEG
APPROACH SPEED	241 km/HR (130 KN)	241 km/HR (130 KN)
INITIAL CRUISE ALTITUDE	10,394 m (34,100 FT)	10,485 m (34,400 FT)
TAKEOFF FIELD LENGTH AT SL, 84°F	2286 m (7500 FT)	2362 m (7750 FT)
WING AREA	208 SQ m (2242 SQ FT)	209 SQ m (2255 SQ FT)
PARASITE DRAG EQUIVALENT FLAT PLATE AREA	3.880 SQ m (41.776 SQ FT)	3.808 SQ m (40.985 SQ FT)
ASPECT RATIO	10.85	8.24
MISSION RESULTS		
750-N-MI MISSION		
BLOCK TIME	2.021 HR	2.022 HR
BLOCK FUEL	8275.7 kg (18,245 LB)	8151.9 kg (17,972 LB)
CONSTANT ALTITUDE	11,278 m (37,000 FT)	11,278 m (37,000 FT)

SIZING AND PERFORMANCE RESULTS FOR BASELINE AND WING-WINGLET AIRCRAFT

Direct Operating Cost Evaluation. Direct operating cost (DOC) was calculated in 1978 dollars with a fuel cost of 13 cents per liter (50 cents per gallon). Maintenance cost estimates were based on the first 5 years average. An aircraft productivity of 1.852 million km (1 million n mi) per year was assumed. A 16-year depreciation period with a residual value of 0.16 of the original cost was employed. Development costs were estimated to be $754.26 million for the baseline aircraft and $755.15 for the wing-winglet configuration, with the latter including $5 million for specific winglet development. The development costs were distributed over 400 aircraft. The total cost was $23.902 million for the baseline aircraft, and $23.842 million for the wing-winglet aircraft.

The optimized wing-winglet aircraft consumed 1.5 percent less fuel than the conventional-wing aircraft, and had a DOC 0.7 percent lower ($4182.95 per flight compared to $4211.32). Increases in fuel cost over the conservative figure used in the analysis would increase the DOC difference. For a fuel cost of 26 cents per liter ($1 per gallon), the DOC benefit of the wing-winglet aircraft would be 0.9 percent. A further fuel cost rise to 52 cents per liter ($2 per gallon) would apparently increase the benefit to 1.08 percent; however, this figure should be regarded as approximate since such fuel costs would be expected to have indirect effects on other costs in the DOC calculation.

The DOC benefit figures are significant enough to warrant further investigation of the concept, particularly in the structural area which was shown to be sensitive.

RELAXED STATIC STABILITY AND AUGMENTATION SYSTEM STUDY*

Objectives

The prime objective was to define the system required to augment the relaxed static stability of the baseline aircraft.

Subsidiary objectives were:

- The definition of design constraints for flying qualities and criteria for reliability and safety such that the aircraft could be flown and landed safely in the event of failure of the system
- The evaluation of competing system concepts
- The assessment of the impact of the concept on the aircraft certification task.

Approach

Using the variations on baseline aircraft definition, a flying-qualities evaluation was conducted on a motion-base simulator. The results established a relationship of flying qualities to longitudinal configurations for the aircraft. Fuel savings were determined for the acceptable configuration.

Augmentation control laws were developed using the conventionally stable DC-10 aircraft as the flying-qualities model.

A flying-qualities evaluation of selected control laws was performed on the motion-base simulator. The evaluation established the flying-qualities improvement over the unaugmented aircraft and examined failure-reversion effects.

---

*The contract study is reported in detail in the document of Reference 5.

The augmentation system functional design was accomplished, including definition of the major system elements. Candidate architectures were formulated and evaluated. A complete reliability analysis was performed on the selected systems.

Finally, the pertinent FAA regulations were listed, a validation plan proposed, and a typical airframe manufacturer's cost (including RSSAS hardware) estimated.

Benefits of Relaxed Static Stability

The benefit of relaxed static stability for the EET was shown by a parametric study. One configuration, having an aerodynamic center margin at aft center of gravity of 10 percent, represented currently conventional levels of natural longitudinal stability. Another represented the baseline aircraft, having neutral stability. A third was configured with marked natural instability, having −14.3 percent margin. The fuel savings relative to the conventional configuration are shown here.

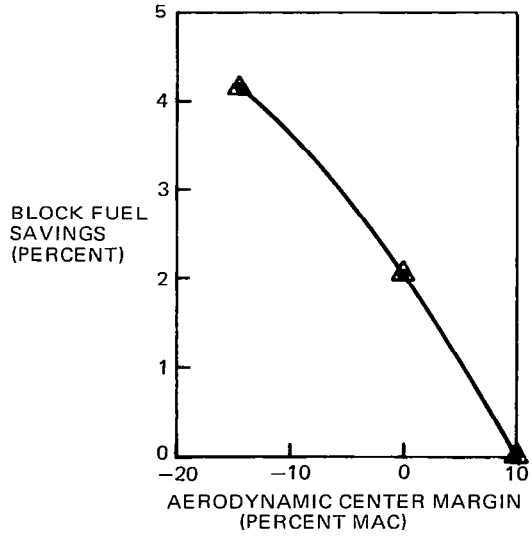

FUEL SAVINGS FROM PARAMETRIC STUDY

From the study evaluations, a recommendation for the precise amount of tolerable natural instability was developed.

Flying Qualities Criteria

Criteria were defined to specify the flying qualities that would be acceptable in the event of total augmentation system failure, and to establish the qualities desired with the augmentation system in normal operation.

The flying qualities were described in terms of both Cooper-Harper pilot rating values and the military flying quality "levels". Safety considerations for commercial transport aircraft in the case of the unaugmented aircraft dictate a maximum acceptable pilot rating of 6.5, which corresponds approximately to the boundary for Level 2 from the military specification. The desired flying qualities of the normal augmented aircraft are those of military Level 1, which corresponds to a pilot rating of 3.5 or better.

It was decided that Level 1 flying qualities for the augmented vehicle could be ensured by requiring the augmentation system to provide a match with the proven good qualities of the DC-10. In addition, the "bandwidth model" pitch-tracking criterion was employed.

Motion-Base Simulator Tests

The simulations of the aircraft and of the RSSAS were conducted on the Douglas 6-degree-of-freedom motion simulator. This mechanism supports a complete simulated transport cockpit and provides realistic motion cues.

In the first simulation, flying qualities of the unaugmented aircraft were examined through most of the flight envelope with emphasis placed on the cruise flight and landing approach. Ratings were obtained from five test pilots for a number of configuration variations and in conditions of turbulence or calm. In the second simulation, flying qualities of the augmented aircraft were examined by six test pilots in landing approach and cruise. Some reversion conditions were examined, together with configuration variations and turbulence.

Mean (average) pilot ratings were used to define the trends of the data. Two interpretations of the results were made. One weighted the data at each test point equally to produce a true mean of the pilot ratings. The other interpretation reflected the worst average in the sample, so the average would represent what may be a significant portion of the airline pilot population. The conservative interpretation was used for presentations on pilot ratings, and for estimating fuel savings.

For the landing approach cases, the RMS vertical gust intensity of the turbulence model was 2.13 m/s (7.0 ft/sec). Pilots described this level as "moderate" or "moderate to heavy." It is believed that the intensity would be more accurately described as "heavy" or "severe" if the full motion cues were felt by the pilot without the attenuation inherent in a ground-based simulator. For the cruise condition, the RMS turbulence value was 1.5 m/s (5.0 ft/sec), generally described as "moderate."

Tests of the Unaugmented Configurations. The effect of static margin on mean pilot rating for the landing approach task in turbulence is shown below. The solid curve considers all the means, and the dashed line considers only the worst of the means. The minimum acceptable static margin was minus 2.5 percent MAC. This margin expressed as aerodynamic center margin was minus 3.1 percent MAC. The corresponding minimum time-to-double-amplitude was approximately 7 or 8 seconds, depending on the tail area.

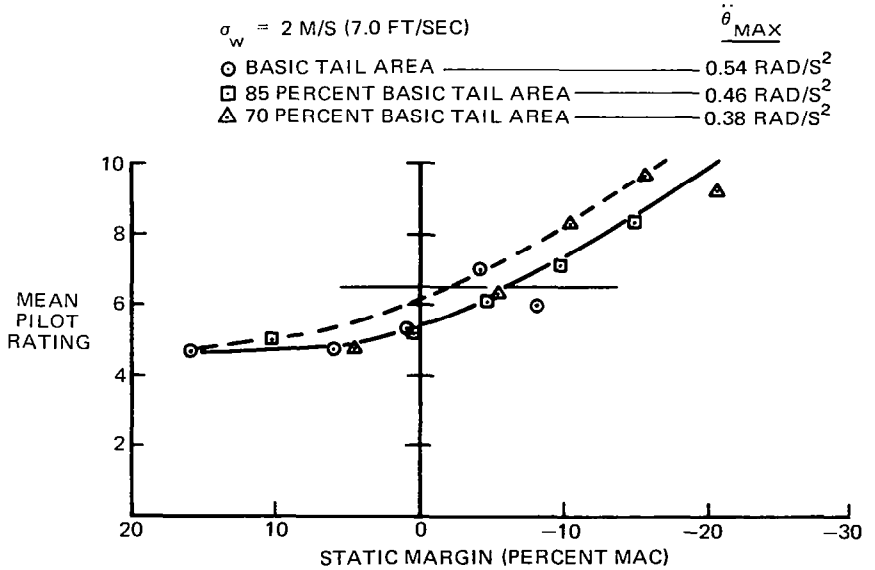

EFFECT OF LONGITUDINAL STABILITY ON MEAN PILOT RATING – LANDING APPROACH

Variations in tail size did not result in specific comments over the stability range of interest. The effect of flying in calm air reduced the ratings by approximately one unit for the stable cases and two units for the unstable cases.

Agreement between pilot ratings and the boundaries of the pitch tracking criterion was generally good, particularly near the Level 2 boundary. The ratings near the Level 1 boundary were worse then expected, probably because of poor lateral-directional characteristics incorporated at that time in the model.

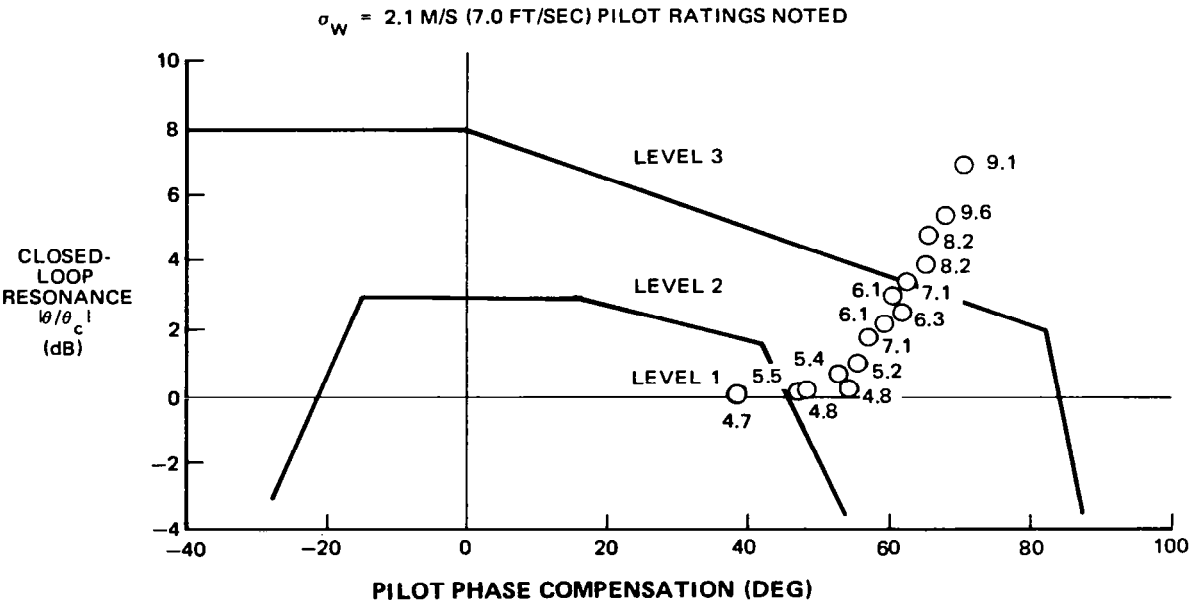

PITCH-TRACKING CRITERION – LANDING APPROACH

For the unaugmented cruise flight condition, maneuver margin was chosen as the metric of stability rather than static margin. Maneuver margin is more appropriate for this condition, in which load factor changes provide important cues for the pilot. The minimum acceptable maneuver margin for a pilot rating of 6.5 is approximately minus 1 percent MAC. The effect of calm air was small, reducing the pilot ratings by less than half a unit for the stable cases and by nearly one unit for the unstable cases. This small effect is attributed to the rather low precision required in the cruise piloting task.

The cruise maneuver margin limit equated to minimum acceptable aerodynamic center stability level of about minus 4.5 percent MAC. This figure was used to determine the mission fuel savings due to relaxed static stability. The savings, which are significant, were 2.8 percent relative to an aircraft of conventional design, and three-quarters of 1 percent relative to the baseline which had neutral stability.

Tests of the Augmented Aircraft. The tests examined the flying qualities resulting from the application of three control laws, certain augmentation system features, and several reversion conditions. Evaluations were also made of various levels of augmentor elevator authority, auto trim failure, thrust compensation failure, passive total failure of each of the augmentors, and augmentor failures in which reversion from one control law to another occurred.

For these tests, the previously troublesome lateral-directional characteristics were improved by an increase in lateral control sensitivity for small deflections. Pilot commentary confirmed that the characteristics were considerably improved, but the pilot ratings did not reflect a significant change. It is believed that the pilots in the first test had attempted to overlook the deficiencies when rating the longitudinal properties. Checks of the unaugmented aircraft supported the previous results defining the allowable static and maneuver margin.

Augmentors (control laws) No. 1, No. 3, and No. 5 were evaluated in the landing approach in the presence of turbulence. The pilot ratings for each averaged 3.8 for the aft cg location of 40-percent MAC. The comparable rating for the unaugmented aircraft was 6.0. In cruise flight, only augmentor No. 5 was evaluated. Because the unaugmented aircraft was rated satisfactory in this flight condition, there was little room for improvement, and none was observed.

Large elevator deflections in go-around were required because of the pitching moment resulting from the engine thrust change. They could be trimmed out if unaugmented, or satisfied by the augmentor. Augmentation significantly reduced the magnitude of the required command. Authority-limiting during go-around had the effect of allowing more of the natural pitching moment due to the thrust change. Some limitation was found unobjectionable. With no augmentor, however, the go-around pitch required immediate and constant pilot attention. This indicates that the amount of lead in the initial command is more important than authority.

Simulated auto trim failure was handled acceptably. However, the concept of a "trim director" is unusual, and detail development is required to minimize pilot workload in this area.

Passive total failure of each of the augmentors did not degrade the flying qualities below those of the basic aircraft. Transition from one control law to another was unobjectionable.

Reliability and Safety

The reliability goals for the stability augmentation system were based on those of the comparable systems of the DC-10. The EET components were in most cases similar or identical to those used on the DC-10. The major differences were in the flight guidance system where a greater degree of functional integration was used, in the primary control elevator and stabilizer trim actuation, and in the addition of the augmentation system.

Reliability. The required system capability was specified with three terms:

- Dispatchability — The minimum capability required to begin a mission.
- Mission Reliability — The probability the system will not cause an abort in flight.
- Economic Reliability — The frequency of maintenance actions on the system components.

Dispatchability is defined by the probability that a scheduled flight will not be delayed or cancelled due to equipment malfunctions. The DC-10 dispatchability record for a typical year, representing all events affecting departures and flights attributed to the aircraft systems being compared, was approximately 1 event per 330 departures. A goal of 3×10^{-3} was thus established as the dispatchability probability for the new configuration including the addition of RSSAS functions.

Mission reliability is the probability that a flight after takeoff will continue to its planned destination. The DC-10 data record indicated that none of the recorded aborts were justified as required by the aircraft system or hardware state, but were based on pilot judgment of the situation. Although pilot judgment will continue to produce aborts for similar reasons for any new aircraft, it is anticipated that improved fault detection and monitoring should reduce the frequency by providing the crew with better information. From the data, a figure of 5 aborts in 100,000 flights was derived. This figure was subjected to adjustment for safety criteria and design contingency considerations.

Mean time between unscheduled removals (MTBUR) is often used as an indicator of economic reliability because it indicates the frequency of maintenance actions performed on a system. The DC-10 figure for the related system was close to 70 hours, and this was used as the goal for the new system.

Safety. Various approaches are in use among civil and military agencies for controlling the safety level of active or augmented primary control systems. Although a comparison of standards between the various approaches is somewhat subjective, uniformity of philosophy exists. The quantitative scale selected was most conservative; it was based on the CAA/JAR (British Civil Aviation Authority and European Joint Airworthiness Regulations) scale. Therefore, since the unaugmented EET was designed to exhibit Level 2 or better flying qualities for all flight regimes, the probability of functional failure of the augmentation system should be in the area of 1×10^{-5} for 1 hour of flight. Design contingency considerations were used to adjust this figure.

Design Contingency Considerations. The desired functional availability of the RSSAS was based on the traditional capabilities of similar devices such as yaw damping, resulting in a failure rate of 2.5×10^{-6} failures/hour. As a design contingency, it was anticipated that future investigations may determine isolated aircraft/envelope combinations in which the unaugmented aircraft flying qualities degrade to a Level 3. The regulatory requirements would then specify a total RSSAS failure probability of 1×10^{-7} in these flight regimes. This most restrictive system failure probability was established as the reliability requirement for RSSAS design.

Reliability Analysis. The two candidate RSSAS architectures differed only in the redundancy of the flight augmentation computer, one using three computers and the other only two. Two standards for the flight control system technology were evaluated — one with the DC-10 automatic flight guidance system, the other with a new digital system as expected for the EET.

The results of the analysis to determine the probability of function loss showed that even for the worst-case minimum-equipment dispatch, the safety goal of 1×10^{-5} failure probability was not exceeded.

EVENT	BASE DC-10	*RSSAS ADDED 3-COMP CONF	*RSSAS ADDED 2-COMP CONF	*RSSAS AND NEW FGS FUNCTION ADDED	
				3-COMP CONF	2-COMP CONF
DELAYS					
0-15 MIN	0.73×10^{-3}	0.66×10^{-3}	0.89×10^{-3}	0.57×10^{-3}	0.76×10^{-3}
> 15 MIN	2.11×10^{-3}	1.99×10^{-3}	2.38×10^{-3}	1.73×10^{-3}	2.18×10^{-3}
CANCELLATIONS	0.12×10^{-3}	0.11×10^{-3}	0.14×10^{-3}	0.11×10^{-3}	0.13×10^{-3}
ABORTS	0.05×10^{-3}**	———	———	———	———
OUT OF SERVICE	0.02×10^{-3}	0.02×10^{-3}	0.02×10^{-3}	0.02×10^{-3}	0.03×10^{-3}
TOTAL	3.03×10^{-3}	2.79×10^{-3}	3.43×10^{-3}	2.43×10^{-3}	3.10×10^{-3}
MTBUR	(STUDY GOAL) 70 HOURS	76 HOURS	78 HOURS	116 HOURS	122 HOURS

*VALUES BASED ON 1-HOUR FLIGHT; NO CREDIT FOR GROUND REPAIR TIME; TWO COMPUTERS REQUIRED FOR DISPATCH.

**PILOT ELECTIVE ABORTS, NO CRITICAL FUNCTIONS LOST.

RESULTS OF DISPATCH DELAY AND ECONOMIC RELIABILITY ANALYSES

Control Law Development

Control laws were designed for two functions — relaxed longitudinal static augmentation and compensation for pitch coupling to variations in engine thrust. The RSSAS must perform this task by sensing the primary control inputs and aircraft response and by providing supplementary aircraft control commands. The control law design was based on use of the sensors presently available for the DC-10, and duplication of the DC-10 flying qualities with regard to aircraft response to pilot control inputs. The laws were generated from aircraft equations of motion, using modern control analysis techniques and simulation. Thirty-two laws were generated for investigation.

1.	$\theta\ \dot{\theta}\ u\ \alpha$	12.	$\theta\ \dot{\theta}\ A_N\ \dot{h}$	23.	$A_X\ A_N\ \alpha$
2.	$\theta\ \dot{\theta}$	13.	$\theta\ \dot{\theta}\ A_N\ \alpha$	24.	$A_X\ A_N$
3.	$\theta\ \dot{\theta}\ \alpha$	14.	$\theta\ \dot{\theta}\ A_N\ u$	25.	A_X
4.	$\theta\ \dot{\theta}\ u$	15.	$\theta\ \dot{\theta}\ \dot{h}\ u$	26.	A_N
5.	α	16.	$\theta\ \dot{\theta}\ \dot{h}$	27.	$u\ \dot{\theta}$
6	$u\ \alpha$	17.	$A_X A_N\ \dot{h}\ u$	28.	$\alpha\ \dot{\theta}$
7.	u	18.	$A_X\ A_N\ \dot{h}$	29.	$\theta\ \dot{\theta}\ A_N$
8.	$\theta\ \dot{\theta}\ A_X\ A_N$	19.	$\dot{h}\ u$	30.	$A_N\ U$
9.	$\theta\ \dot{\theta}\ A_X\ \alpha$	20.	$\dot{h}$	31.	$A_N\ \dot{h}$
10.	$\theta\ \dot{\theta}\ A_X\ u$	21.	$A_X\ A_N\ u$	32.	$A_N\ \alpha$
11.	$\theta\ \dot{\theta}\ A_X\ \dot{h}$	22.	$A_X\ A_N\ u\ \alpha$		

CONTROL LAWS INVESTIGATED

After preliminary investigation, a number of laws were eliminated, leaving seven (Numbers 1 through 7). The block diagram for all the control laws is shown below. Laws containing A_X (longitudinal acceleration) provided unacceptable response for throttle inputs. Laws containing h (altitude rate) were unable to provide satisfactory performance in turbulence. Laws utilizing $\dot{\theta}$ (pitch rate) without pitch were rejected in favor of others having these parameters. Two laws were eliminated because their combinations of sensors in failure reversion patterns were unsatisfactory.

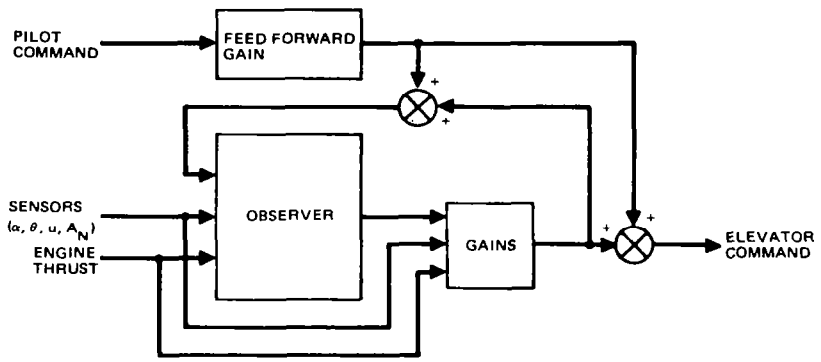

RSSAS CONTROL LAW BLOCK DIAGRAM

The selected laws were shown to provide satisfactory matching of DC-10 characteristics for short-period damping, phugoid, and stability. However, the laws could not accommodate the thrust upset effects, and therefore the addition of thrust/pitch compensation was required.

Three control laws, No. 1 (pitch angle, pitch rate, velocity, angle of attack), No. 3 (pitch angle, pitch rate, angle of attack), and No. 5 (angle of attack) were demonstrated on the motion-base simulator. During the tests, the higher values of pitch and normal acceleration response for law No. 5 manifested themselves with pilot opinions of a more active aircraft. Law No. 1 had the tightest pitch angle control as affirmed by pilot comments. None of the three laws was distinguishable in terms of pilot rating.

System Architecture

The RSSAS consists of sensors to describe the aircraft response, flight augmentation computers to perform the control calculations to achieve the desired flight response, an actuation system which transforms the computations into longitudinal aircraft control, and hydraulic and electrical systems to provide the necessary power. Operationally, the system is independent of other normal aircraft flight controls and will function continuously in conjunction with either pilot or automatic pilot control. Aircraft control is accomplished through the elevator surfaces whose augmentation commands are summed with the primary flightpath commands to provide a total surface deflection. Primary control commands are reflected back to the control column, but the RSSAS control command is not.

In order to meet the contingency failure probability requirement, the system was partitioned into functional subsets.

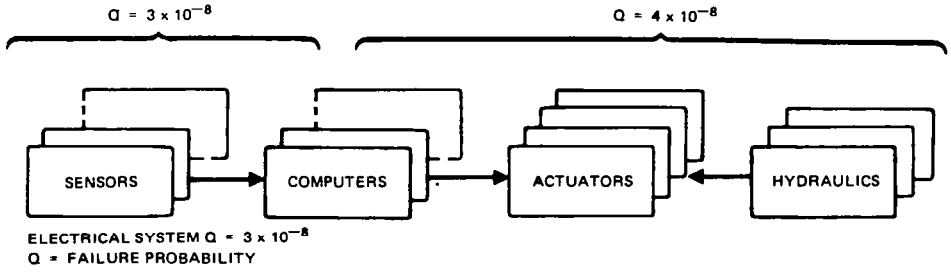

RSSAS FUNCTIONAL PARTITION AND RELIABILITY ASSIGNMENT

The selected system contained a triple-redundant computer which was combined with two dual series input actuators. Each actuator was supplied from a separate hydraulic system. Sensor data were crossfed between the sensors and computer.

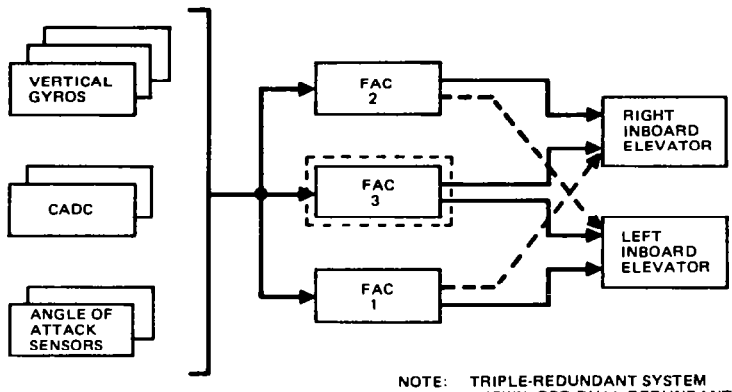

SELECTED RSSAS BLOCK DIAGRAM

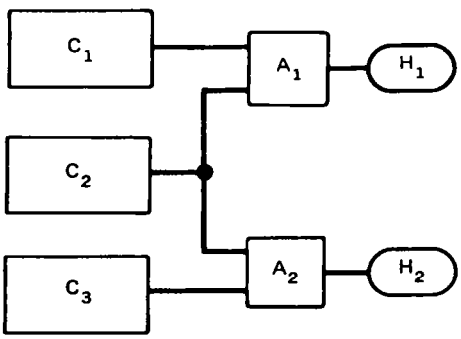

TRIPLE-REDUNDANT COMPUTER/ACTUATOR CONFIGURATION

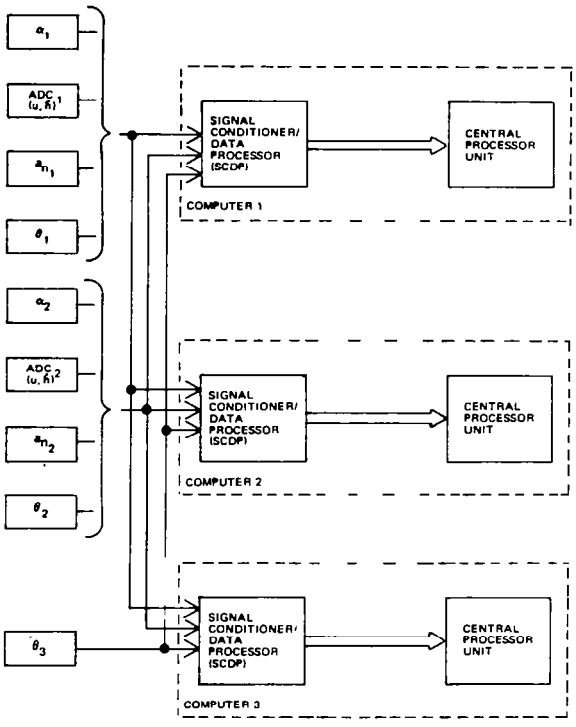

TRIPLE COMPUTER CONFIGURATION

Pitch/thrust compensation was arranged to share computation and actuation devices with the RSSAS. The engine data system was used for sensing.

Since the augmentor is not required for safety of flight, a conventional electrical AC power system without a noninterruptable power source was considered acceptable.

Impact of RSSAS on the Aircraft Design and Certification

Regulatory Requirements. An aircraft with relaxed static stability must comply with certain FAA requirements which specify performance for both the aircraft and augmentation system. The current regulations which relate to the unique stability characteristics of the aircraft were analyzed during the study. It was concluded that the RSSAS could be certified under the current FAR, Part 25.

System Validation. The normal design process includes validation of each element. Validation may include performance compliance, fault-related or system description, and design control. The RSSAS will introduce unique activities in the area of qualitative evaluations of the system or aircraft, which will require additional testing in the simulator and in flight. A typical design and validation program is illustrated.

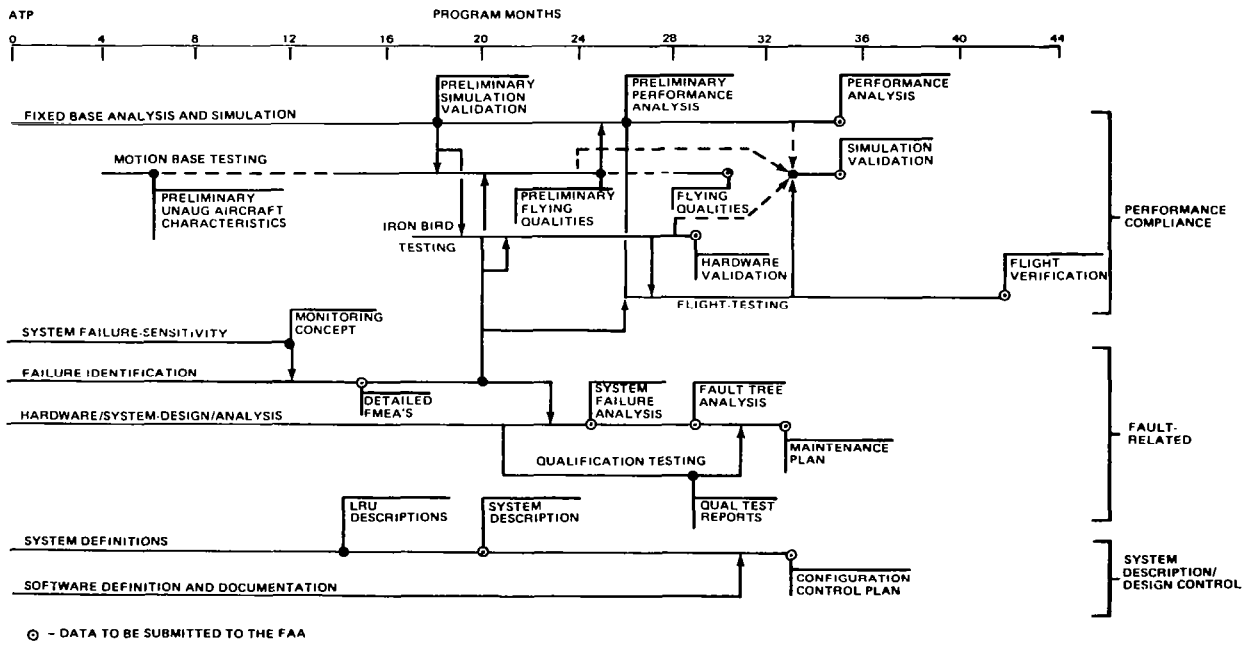

VALIDATION SCHEDULE

RSSAS Implementation Cost. For the purpose of this study, the cost of incorporating the concept in the EET was determined as the differential of the identical aircraft with and without RSSAS. The total nonrecurring airframe manufacturer's cost in 1979 dollars was estimated at $21.75 million. Using a 200-aircraft base to establish the total of nonrecurring and recurring costs, the total cost per aircraft was estimated at $288,750.

AERODYNAMIC PERFORMANCE OF AN AILERON FOR ACTIVE CONTROL

Objective

The objective was to determine the extent to which the outboard ailerons of the DC-10 (designed for low-speed use only) could be used as an active control surface at high and low speeds.

Approach and Results

The program comprised three wind tunnel tests.

The first test was conducted in the NASA Ames Research Center 12-foot high Reynolds number low speed wind tunnel. The purpose of the test was to develop an aerodynamic data base for evaluation of the outboard ailerons for use as active control surfaces. The model was a 4.7-percent-scale DC-10 derivative with an extended span wing and extended span outboard ailerons. The outboard aileron effectiveness was found to be linear and of the expected levels for the range of flap deflections and angles of attack tested. The aircraft pitching moment characteristics with the aileron deflections to be considered for wing load alleviation were well behaved and in the correct direction for good stall recovery characteristics.

The second test was conducted in the Ames Research Center 11-foot transonic tunnel. The purpose of the test was to make a preliminary evaluation at high speed of the outboard ailerons as active control surfaces. The model was a 3.25-percent-scale DC-10 Series 10 transport. The outboard ailerons were found to be promising as effective surfaces for use in a wing load alleviation system. Shock-induced separation was found to occur at Mach numbers above 0.9. Therefore, the satisfactory use of the outboard ailerons for elastic mode control would be subject to further investigation and perhaps development.

The third test was also carried out in the 11-foot transonic tunnel. The purpose of the test was to continue evaluation of the ailerons at high speed. A new model was used — a 3.25-percent-scale derivative DC-10 having an extended wing span and extended fuselage. The outboard ailerons were found to be effective surfaces for use in a wing load alleviation system. Shock-induced separation causing aileron reversal was found to occur at Mach numbers between 0.925 and 0.975. While these Mach numbers were higher than in the second test, it was concluded that configuration changes or development would be required if the ailerons were to be required for elastic mode control.

TECHNOLOGY RECOMMENDATIONS

High-Aspect-Ratio Supercritical Wings

The Phase I program work described in the preceding sections of this report has established a sound technology base for high-aspect-ratio supercritical wings. The results of the studies show the concept to be viable for application to new families of energy-efficient medium-range transports. There are, however, sound reasons why this work should be extended.

The wind tunnel data gained, together with parallel studies for new transports, show that potential still exists for making significant performance gains. In addition, the design work has been extended to an aircraft with a narrower body. It is therefore an objective to examine a new and better wing which benefits from the Phase I program, and reflects the newer direction in configuration. This investigation should be conducted in cruise-speed and high-lift tests. Although a considerable advance in high-lift technology has been made in Phase I, further exploration is recommended before the results are incorporated into the new configuration.

High Speed Aerodynamics. Development in the immediate future should concentrate on the following important problems:

- Drag creep
- Interference of nacelles and pylons.

The investigation of these problems (including related concerns associated with the integrated configuration) is proposed for a wind tunnel program to be conducted in the NASA Ames Research Center 11-foot facility. A new full-span model is proposed.

The Phase I tests showed the inboard wing to be the largest contributor to the drag creep problem. Shocks near the leading edge also contributed. The design of the new model can now benefit from inverse design methods to define modified airfoils to be selected. The resulting performance improvement should also improve the buffet boundary.

Nacelle integration data from Phase I showed low interference in the cruise regime. For the new wing, the nacelles are relatively larger and their behavior requires investigation. Little data exist on the relationship of location with aerodynamic performance and stability.

To explore the characteristics of the new model, two tests are recommended. The first should evaluate the behavior of the new aircraft configuration. The second test should address expansion of technology for this family, including investigation of nacelle integration.

High-Lift Aerodynamics. Development in the immediate future should focus first on the continued investigation of configuration technology on the Phase I model, and then on development of the technology for the new high-speed wing.

Recommended explorations using the Phase I model include:

- Comparison of variable-camber Krueger and slat leading-edge devices
- The use of mixed leading-edge devices
- The requirements for outboard devices offering greater protection
- The effect of spanwise extent of leading-edge devices on stall characteristics
- Evaluation of the fixed-camber Krueger leading-edge device
- Evaluation of a two-segment trailing-edge flap concept

Wind tunnel test programs are proposed. Initial tests are identified for the Langley VSTOL wind tunnel, with follow-on tests at the Ames 12-foot facility.

Experimental evaluation of low-speed characteristics of the new aircraft configuration is recommended in the Ames 12-foot facility.

Wing-Winglet Combination

It is not yet clear what specific recommendations should be made to further this branch of the technology. At this time, no experimental aerodynamics data exist on the combination of a relatively high-aspect-ratio supercritical wing and a winglet. It would

therefore be desirable to introduce aerodynamic wind tunnel explorations of the high-speed and high-lift characteristics of such a combination. It has not yet been found possible to identify how such a program could be arranged economically in the light of more direct priorities. Furthermore, it appears that the evolving technology in active controls may offer potential advantages for the configuration of a wing-winglet combination. The proper study of configurations, including aerodynamic, structural, and integration aspects, should include the effect of such potential, as well as the findings of the next stage of supercritical wing development.

Active Controls

The benefits that may derive from the use of active controls to augment performance, and the principles involved in the use of the concept, have been understood for some time. However, only recently has sufficient work been accomplished to suggest ways by which certain of the modes of active controls may be applied to transport aircraft in the near term. One mode is relaxed static stability augmentation. The depth of work summarized in this report is considered sufficient to support the application of this mode to a new transport.

Technology development associated with wing load alleviation is also encouraging. One area in which more detailed investigation appears necessary is the relationship of a wing active control system on flutter characteristics. An understanding of this relationship opens up the opportunity for elastic mode control in which the capability of the control system results in a more efficient aircraft. It may be possible to utilize elastic mode control to some extent for aircraft in the near term.

The success of elastic mode control depends on a clear understanding of structural, servo control, electronic, and aerodynamic aspects. Experience in active systems has been limited to controlling the rigid-body modes of the aircraft. It is therefore recommended that a program be instituted to develop and confirm flutter analysis methods and gust load alleviation methods.

The program would utilize a dynamic model of a DC-10 derivative having an extended-length fuselage and increased wing span. The outboard aileron and perhaps the inboard elevator would be actively controlled. Control laws for suppressing flutter and reducing wing bending loads due to gust are required. It is proposed that an initial test in the Douglas-Long Beach low-speed wind tunnel be conducted using a semispan model. A full-span test would be conducted in the Northrop 7- by 10-foot wind tunnel. Correlation of test results with analytical predictions would then be made.

Following the completion of this program, further recommendations for technology development would be made so that the maximum benefit could be shown from active controls. It is believed that additional investigations should include the use of the technology on promising unconventional configurations, particularly the wing-winglet combination.

REFERENCES

1. Steckel, D.S.; Dahlin, J. A.; and Henne, P.A.: Results of Design Studies and Wind Tunnel Tests of High-Aspect-Ratio Supercritical Wings for an Energy Efficient Transport. NASA CR-159332, October 1980.

2. Oliver, W. R.: Results of Design Studies and Wind Tunnel Tests of an Advanced High Lift System for an Energy Efficient Transport. NASA CR-159389, December 1980.

3. Shollenberger, C.A.: Application of an Optimized Wing-Winglet Configuration to an Advanced Commercial Transport. NASA CR 159156, November 1979.

4. Gilkey, R.D.: Design and Wind Tunnel Tests of Winglets on a DC-10 Wing. NASA CR 3119, April 1979.

5. Sizlo, T.R.; Berg, R.A.; and Gilles, D. L.: Development of a Low-Risk Augmentation System for an Energy Efficient Transport having Relaxed Static Stability. NASA CR-159155, December 1979.

1. Report No.	2. Government Accession No.	3. Recipient's Catalog No.
NASA CR-3469		

4. Title and Subtitle	5. Report Date
SELECTED ADVANCED AERODYNAMIC AND ACTIVE CONTROL CONCEPTS DEVELOPMENT - SUMMARY REPORT	October 1981
	6. Performing Organization Code ACEE-06-FR-0290

7. Author(s)	8. Performing Organization Report No.
The Staff of Douglas Aircraft Company	
	10. Work Unit No.

9. Performing Organization Name and Address	11. Contract or Grant No.
Douglas Aircraft Company McDonnell Douglas Corporation 3855 Lakewood Boulevard Long Beach, California 90846	NAS1-14744
	13. Type of Report and Period Covered Contractor Report

12. Sponsoring Agency Name and Address	14. Sponsoring Agency Code
National Aeronautics and Space Administration Washington, D.C. 20546	

15. Supplementary Notes

Langley Technical Monitors: Donald L. Maiden and Dennis W. Bartlett
Final Report

16. Abstract

A task for the Energy Efficient Transport program conducted (1) The design and wind tunnel development of high-aspect-ratio supercritical wings, investigating the cruise speed regime and also high-lift. (2) The preliminary design and evaluation of an aircraft combining a high-aspect-ratio supercritical wing with a winglet. (3) Active Controls: The determination of criteria, configuration, and flying qualities associated with augmented longitudinal stability of a level likely to be acceptable for the next generation transport; and the design of a practical augmentation system. The baseline against which the work was performed and evaluated was the Douglas DC-X-200 twin engine derivative of the DC-10 transport. The supercritical wing development showed that the cruise and buffet requirements could be achieved and that the wing could be designed to realize a sizable advantage over today's technology. Important advances in high lift performance were shown. The design study of an aircraft with supercritical wing and winglet suggested advantages in weight and fuel economy could be realized. The study of augmented stability, conducted with the aid of a motion base simulator, concluded that a negative static margin was acceptable for the baseline unaugmented aircraft. Simple control laws were found adequate to supply the required flying qualities for the augmented aircraft. Additional work related to active controls determined the performance and potential limitations of existing ailerons on the DC-10 transport when considered for use as a wing load alleviation device.

17. Key Words (Suggested by Author(s))	18. Distribution Statement
Aircraft Energy Efficiency Supercritical Wings High Lift Winglets Augmented Stability Active Controls	FEDD Distribution Subject Category 02

19. Security Classif. (of this report)	20. Security Classif. (of this page)	21. No. of Pages	22. Price
Unclassified	Unclassified	78	

Available: NASA's Industrial Applications Centers

NASA-Langley, 1981